An ionization region model of the reactive Ar/O_2 high power impulse magnetron sputtering discharge

Jón Tómas Guðmundsson[1,2]

[1] Division of Space and Plasma Physics,
KTH Royal Institute of Technology, Stockholm, Sweden
[2] Science Institute, University of Iceland, Reykjavik, Iceland

Department of Physics, University of West Bohemia,
Pilsen, Czech Republic
April 3., 2025

Introduction

- Magnetron sputtering discharges are widely used in thin film processing

- Applications include
  - thin films in integrated circuits
  - magnetic material
  - hard, protective, and wear resistant coatings
  - optical coatings
  - decorative coatings
  - low friction films

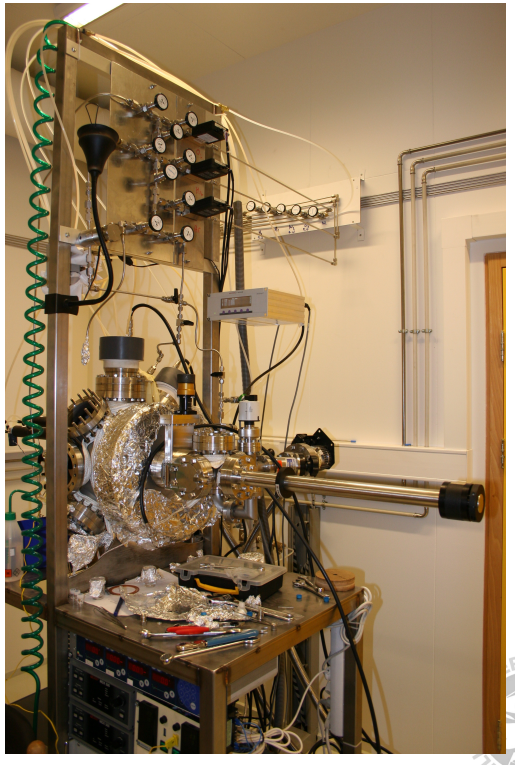

Introduction

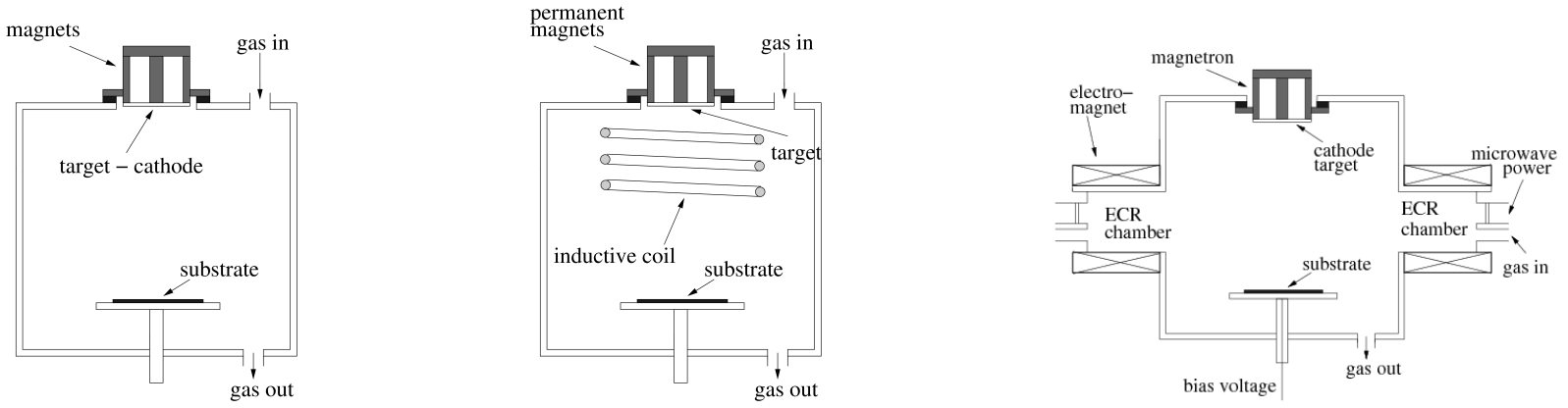

From Gudmundsson (2008), J. Phys.: Conf. Ser. **100** 082002

- A typical dc planar magnetron discharge operates at a pressure of 0.5 – 2 Pa with a magnetic field strength of 10 – 50 mTesla and at cathode potentials 300 – 700 V
- Electron density in the substrate vicinity is in the range $10^{15} - 10^{16}$ m^{-3}
  - low fraction of the sputtered material is ionized ($\sim$ 1 %)
  - the majority of ions are the ions of the inert gas
  - additional ionization by a secondary discharge (rf or microwave)

Introduction

- Often high ionization of the sputtered species is desired – which requires very high density plasma
- In a conventional dc magnetron sputtering discharge the power density (plasma density) is limited by the thermal load on the target
- High power pulsed magnetron sputtering (HPPMS)
- In a HiPIMS discharge a high power pulse is supplied for a short period
  - low frequency
  - low duty cycle
  - low average power

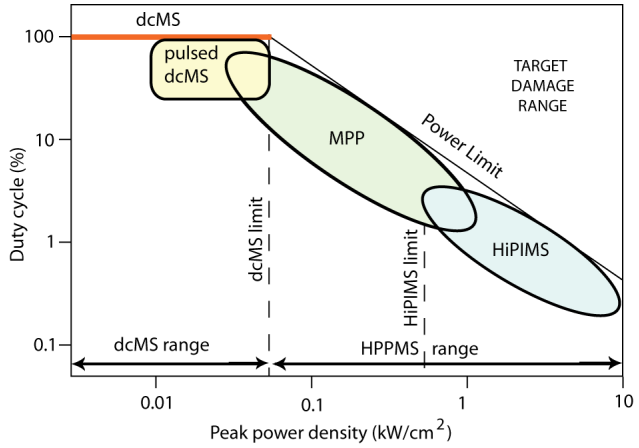

Gudmundsson et al. (2012), JVSTA **30** 030801

- Power density limits
  $p_t = 0.05$ kW/cm^2 dcMS limit
  $p_t = 0.5$ kW/cm^2 HiPIMS limit

Introduction

- Reactive sputtering, where metal targets are sputtered in a reactive gas atmosphere to deposit compound materials is of utmost importance in various technologies
- In reactive sputtering processes a reactive gas O_2, N_2, or CH_4 etc. is mixed to the noble working gas for oxide, nitride, or carbide deposition
- HiPIMS deposition generally gives denser, smoother films and higher crystallinity than dcMS grown films

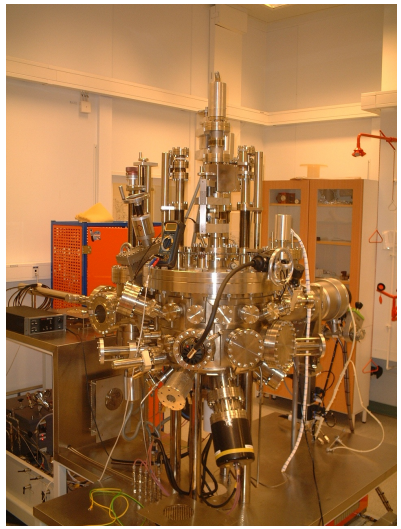

Helmersson et al. (2006) Thin Solid Films **513** 1

Magnus et al. (2012) IEEE EDL **33** 1045

Reactive HiPIMS - Applications

Application – Film Resistivity

- TiN as diffusion barriers for copper and aluminum interconnects
- HiPIMS deposited films have significantly lower resistivity than dcMS deposited films on SiO_2 at all growth temperatures due to reduced grain boundary scattering
- Thus, ultrathin continuous TiN films with superior electrical characteristics and high resistance towards oxidation can be obtained with HiPIMS at reduced temperatures

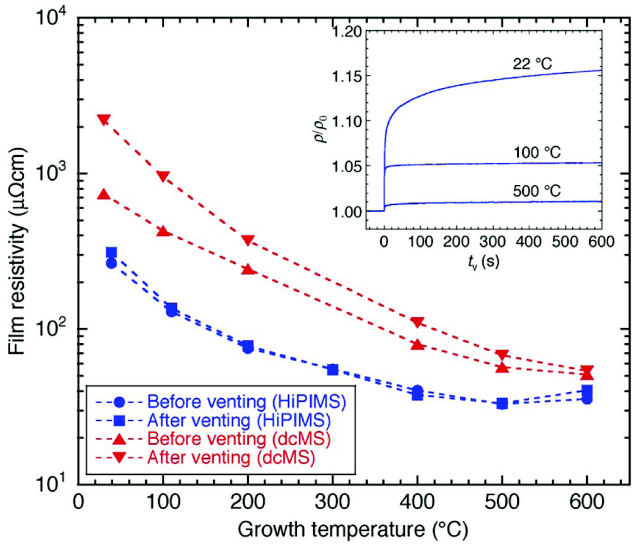

From Magnus et al. (2012) IEEE EDL **33** 1045

Application – Bragg mirror

- Multilayer structures containing a high-contrast (TiO_2/SiO_2) Bragg mirror
- fabricated on fused-silica substrates
  - reactive HiPIMS TiO_2 (88 nm)
  - reactive dcMS SiO_2 (163 nm)
  - capped with semitransparent gold
- Rutile TiO_2 (n = 2.59) and SiO_2 (n = 1.45) provide a large index contrast
- Smooth rutile TiO_2 films can be obtained by HiPIMS at relatively low growth temperatures, without post-annealing

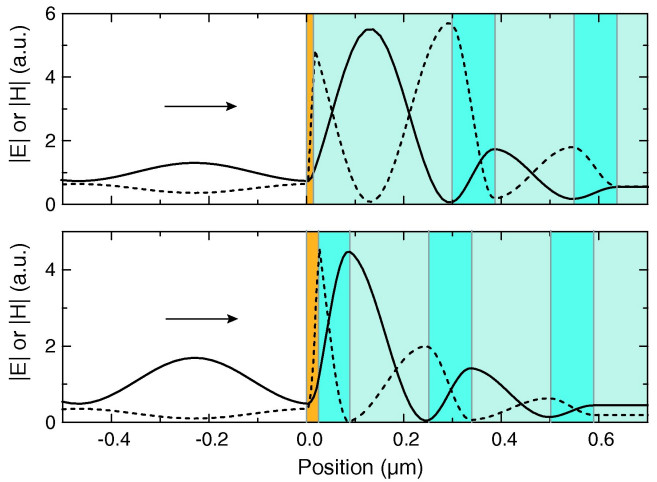

From Leosson et al. (2012) Opt. Lett. **37** 4026

Agnarsson et al. (2013) TSF **545** 445

Voltage - Current - Time characteristics

Non-reactive HiPIMS

HiPIMS - Voltage - Current - time

- To describe the discharge current-voltage characteristics the current-voltage-time space is required
- The early work on HiPIMS used 50 – 100 μs pulses and a pulse repetition frequency in the range 50–1000 Hz
- The applied target voltage V_d and target current I_d for an argon discharge at 0.4 and 2.7 Pa. The target is made of copper 150 mm in diameter

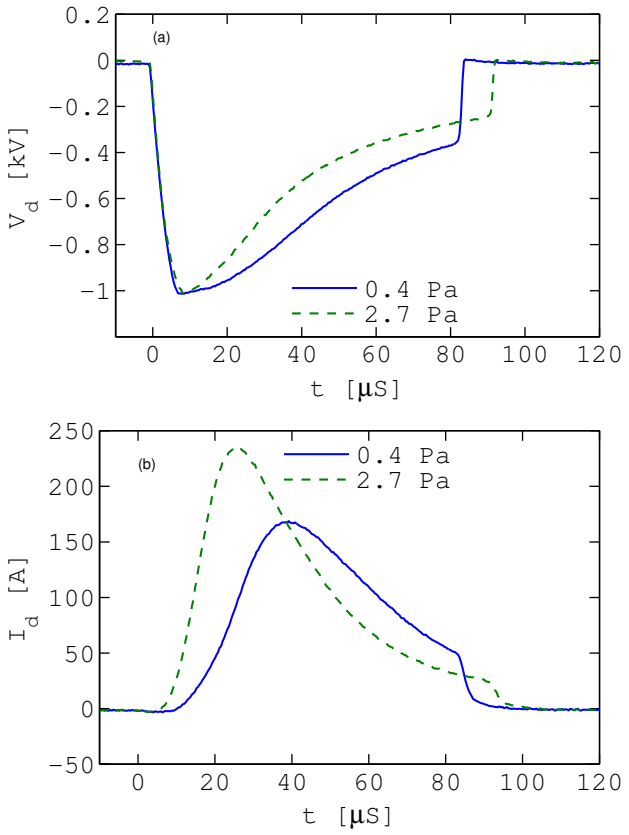

From Gudmundsson et al. (2012), JVSTA **30** 030801

HiPIMS - Voltage - Current - time

- Modern pulser units have large storage capacitor, the voltage pulse V_D on the cathode can be almost square even for high currents I_D during the full pulse length
- A square voltage pulse is achieved as seen in the discharge voltage and current waveforms for Ar/N_2 discharges operated at different nitrogen flow rates while the argon flow rate was kept fixed at 40 sccm to achieve 0.9 Pa and 150 W average power for 200 μs long pulses

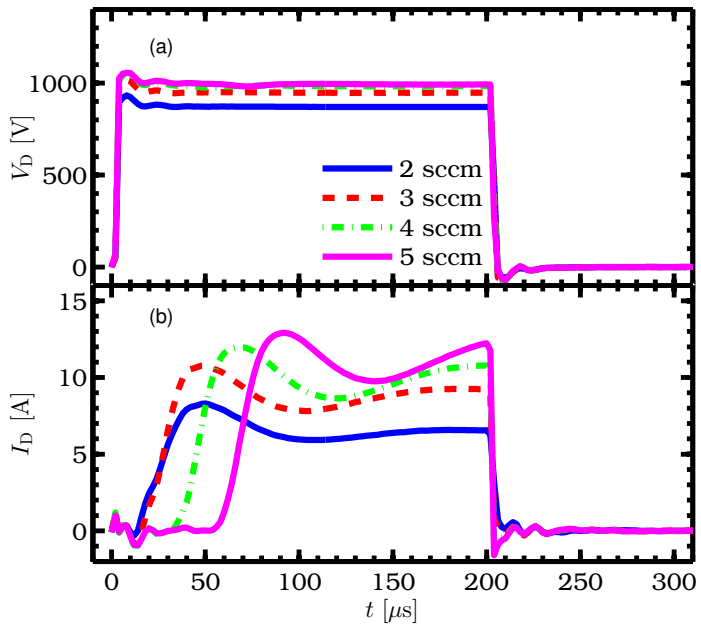

From Hajihoseini and Gudmundsson (2017), JPD **50** 505302

HiPIMS - Voltage - Current - time

- In **non-reactive** discharge the current waveform shows an initial pressure dependent peak that is followed by a second phase that is power and material dependent
- The initial phase has a contribution from the working gas ions, whereas the later phase has a strong contribution from self-sputtering at high voltage

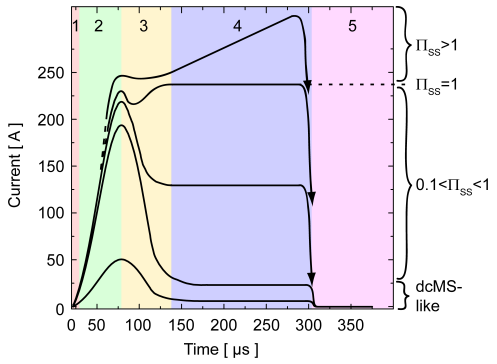

From Gudmundsson et al. (2012), JVSTA **30** 030801

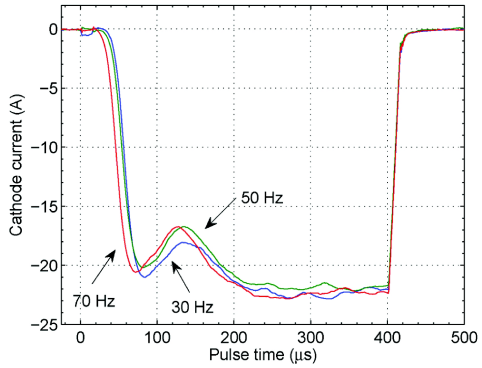

From Magnus et al. (2011) JAP **110** 083306

Ionization region model studies of non-reactive HiPIMS

Ionization region model non-reactive HiPIMS

- The ionization region model (IRM) was developed to improve the understanding of the plasma behaviour during a HiPIMS pulse and the afterglow
- The main feature of the model is that an ionization region (IR) is defined next to the race track
- The IR is defined as an annular cylinder with outer radii r_{c2}, inner radii r_{c1} and length $L = z_2 - z_1$, extends from z_1 to z_2 axially away from the target

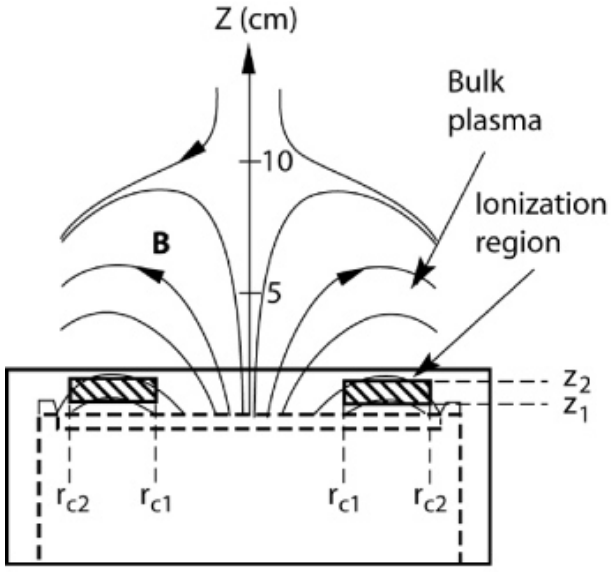

The definition of the volume covered by the IRM

From Raadu et al. (2011), PSST **20** 065007

Ionization region model non-reactive HiPIMS

- The temporal development is defined by a set of ordinary differential equations giving the first time derivatives of
  - the electron energy
  - the particle densities for all the particles
- The species assumed in the non-reactive-IRM are
  - cold electrons e^C, hot electrons e^H
  - argon atoms Ar($3s^2 3p^6$), warm argon atoms in the ground state Ar^W, hot argon atoms in the ground state Ar^H, Ar^m ($1s_5$ and $1s_3$) (11.6 eV), argon ions Ar^+ (15.76 eV)
  - titanium atoms Ti($a\,^3F$), titanium ions Ti^+ (6.83 eV), doubly ionized titanium ions Ti^{2+} (13.58 eV)
  - aluminium atoms Al($^2P_{1/2}$), aluminium ions Al^+ (5.99 eV), doubly ionized aluminium ions Al^{2+} (18.8 eV)

Detailed model description is given in Huo et al. (2017), JPD **50** 354003

Ionization region model non-reactive HiPIMS

- The particle balance equation for a particular species is given by

$$\frac{\mathrm{d}n_{\mathrm{species}}}{\mathrm{d}t} = \sum R_{\mathrm{species,process}}$$

- The reaction rate $R_{j,\mathrm{volume}}$ for a given volume reaction of a species j is

$$R_{j,\mathrm{volume}} = k \times \prod_i n_{\mathrm{r},i} \qquad [\mathrm{m}^{-3}\mathrm{s}^{-1}]$$

- The rate coefficient k for each electron impact reaction is calculated from a given cross section assuming a Maxwellian electron energy distribution
- Two populations of electrons are assumed, the cold electrons created in the bulk ionization processes and hot electrons originating from secondary electrons emitted from the target due to ion bombardment

Ionization region model non-reactive HiPIMS

- For each ion there is a loss rate given as

$$R_{\mathrm{i,loss}} = -\frac{\Gamma_i^{\mathrm{BP}} S_{\mathrm{BP}} + \Gamma_i^{\mathrm{RT}} S_{\mathrm{RT}}}{\mathcal{V}_{\mathrm{IR}}}$$

  where i stands for the particular ion and S_{BP} is the area of the annular cylinder facing the lower density plasma outside the IR (bulk plasma), and Γ_i^{BP} is the flux of ion i across the boundary towards the lower density plasma

- Thus the flux out of the IR towards the lower density plasma is reduced as required to obtain the assumed ion back-attraction probability β

$$\Gamma_i^{\mathrm{BP}} = \left(\frac{1}{\beta} - 1\right) \frac{S_{\mathrm{IR}}}{S_{\mathrm{BP}}} \Gamma_i^{\mathrm{RT}}$$

Ionization region model non-reactive HiPIMS

- In addition there is a change in the neutral density due to kick-out by collisions with fast sputtered atoms coming from the target
- The rate at which species are sputtered off the target (Al, Ti and O) is

$$R_{\mathrm{n,sputt,X}} = \frac{\sum_i \Gamma_i^{\mathrm{RT}} S_{\mathrm{RT}} Y_i(\mathcal{E}_i)}{\mathcal{V}_{\mathrm{IR}}} = \Gamma_{\mathrm{sputter,X}} \frac{S_{\mathrm{RT}}}{\mathcal{V}_{\mathrm{IR}}}$$

and i stands for the ion involved in the process, here $i = M^+$, M^{2+}, Ar^+, O^+, and O_2^+, Γ_i^{RT} is the flux of ion i towards the target

Ionization region model non-reactive HiPIMS

- For each of the neutrals Y of the working gas, including each of the metastable states, the particle balance includes a loss term

$$R_{\mathrm{n,kick-out}} = -\frac{1}{2}\frac{v_{\mathrm{ran},X}}{L} F_{\mathrm{coll,X\rightarrow Y}} \frac{M_X}{M_Y} \frac{\sum n_{X,i}}{\sum_i n_{Y,i}} n_Y$$

- The sum is taken over all the states of that sputtered species and

$$F_{\mathrm{coll,X\rightarrow Y}} = 1 - \exp\left(-L/\lambda_{X,\mathrm{gas}}\right)$$

is the probability of a collision inside the IR, where $\lambda_{X,\mathrm{gas}}$ is the mean free path for an atom X sputtered off the target

Ionization region model non-reactive HiPIMS

- Note that $F_{\mathrm{coll,X\to Y}}$ is the fraction of the momentum carried by the sputtered species that is transferred to the kicked-out species Y
- We can therefore link the sputter flux $\Gamma_{\mathrm{sputter}}$ (in $\mathrm{m^{-2}\ s^{-1}}$) to the kick-out flux $\Gamma_{\mathrm{kickout}}$ out of the IR by

$$R_{\mathrm{kickout,X\to Y}} = F_{\mathrm{coll,X\to Y}}\Gamma_{\mathrm{sputter,X}}\frac{S_{\mathrm{RT}}}{\mathcal{V}_{\mathrm{IR}}} = \Gamma_{\mathrm{kickout}}\frac{S_{\mathrm{DR}}}{\mathcal{V}_{\mathrm{IR}}},$$

- The sputtered flux is

$$\Gamma_{\mathrm{sputter,X}} = \sum_i \Gamma_i^{\mathrm{RT}} Y_i(\mathcal{E}_i)$$

where $Y_i(\mathcal{E}_i)$ is the sputter yield for an ion species i bombarding the target

Barynova et al. (2024) PSST **33**(6) 065010

Ionization region model non-reactive HiPIMS

- Gas rarefaction lowers the density of the working gas inside the IR below the value in the surrounding gas reservoir, $n_{g,0}$
- This gives a back-diffusion (gain) term

$$R_{g,\mathrm{refill}} = \frac{1}{2} v_{\mathrm{ran}} \frac{(n_{g,0} - n_g) S_{\mathrm{RT}}}{\mathcal{V}_{\mathrm{IR}}}$$

where the subscript g stands for the atoms and molecules of the working gas Ar and O_2

Ionization region model non-reactive HiPIMS

- The return flux of recombined positive argon ions Ar^+ from the target is treated as two groups of atoms with different temperatures
  - a hot component Ar^H that returns from the target with a typical energy of a few electron volts
  - a warm component Ar^W that is assumed to be embedded in the target at the ion impact, and then return to the surface and finally leave with the target temperature, at most 0.1 eV
- Thus there is a loss out of the IR

$$R_{\mathrm{Ar^Z,loss}} = -v_{\mathrm{ran}} n_{\mathrm{Ar}^Z} \frac{S_{\mathrm{RT}}}{\mathcal{V}_{\mathrm{IR}}}$$

where Z stands for H for hot or W for warm argon atoms

Ionization region model non-reactive HiPIMS

- The IRM is a semi-empirical model in the sense that it uses a measured discharge current waveform as a main input parameter
- Measured and calculated temporal variations of the discharge current for various discharge (cathode) voltages for a 50 mm diameter Zr target

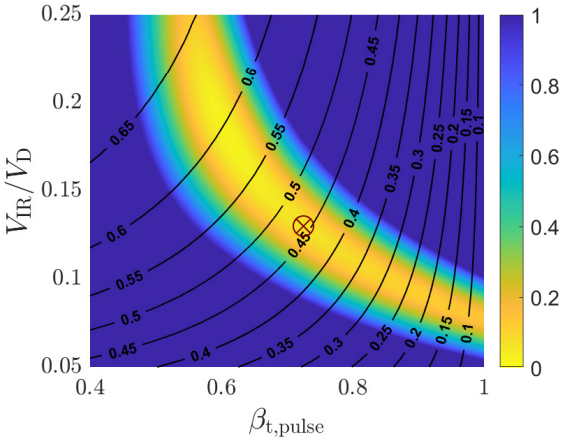

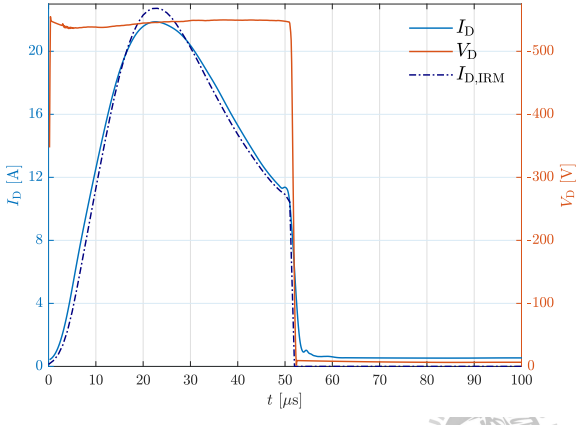

From Suresh Babu et al. (2024) JVSTA **42** 043007

Ionization region model non-reactive HiPIMS

- The model needs to be adapted to an existing discharge (the geometry and pressure, the process gas, sputter yields, target species, and a reaction set for these species) and then fitted to two or three parameters
  - The voltage drop across the IR, V_{IR}, accounts for the power transfer to the electrons
  - The probability of back-attraction of ions to the target β
  - The probability r of back-attraction of secondary electrons emitted
- Sometimes we use the measured ionized flux fraction to lock the model

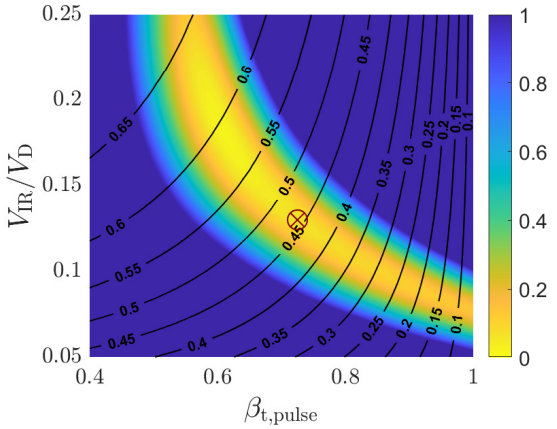

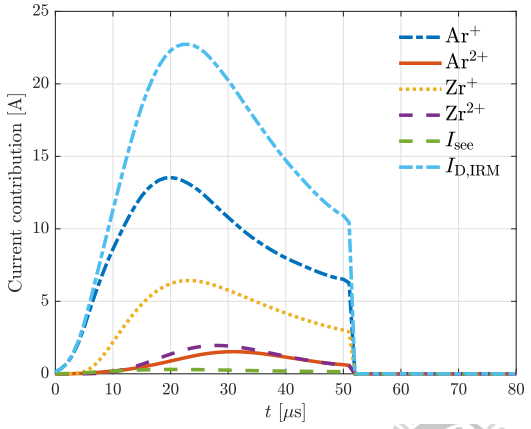

From Suresh Babu et al. (2024) JVSTA **42** 043007

Voltage - Current - Time characteristics

Reactive HiPIMS

HiPIMS - Voltage - Current - time

- During **reactive sputtering**, a reactive gas is added to the inert working gas
- The current waveform in the reactive Ar/N_2 HiPIMS discharge with Ti target is highly dependent on the pulse repetition frequency
- N_2 addition changes the plasma composition and the target condition can also change due to the formation of a compound on its surface

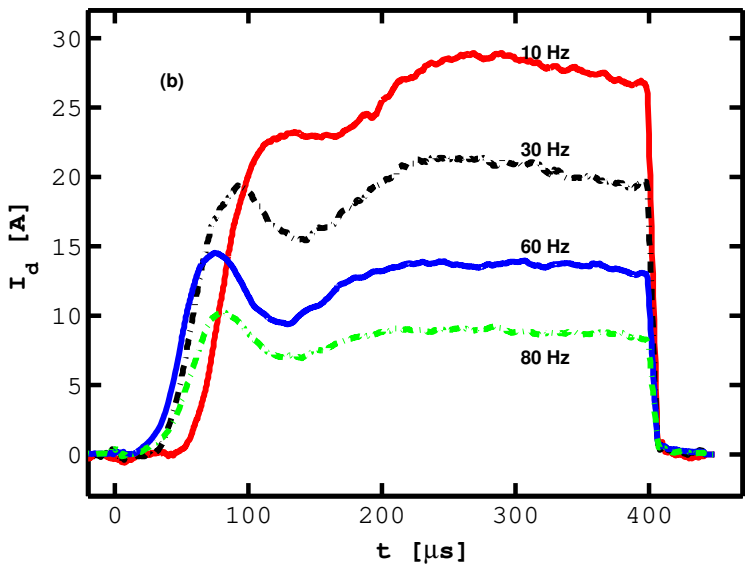

After Magnus et al. (2011) JAP **110** 083306

HiPIMS - Voltage - Current - time

- Similarly for the Ar/O_2 discharge, the current waveform is highly dependent on the repetition frequency and applied voltage which is linked to oxide formation on the target
- The current is found to increase significantly as the frequency is lowered

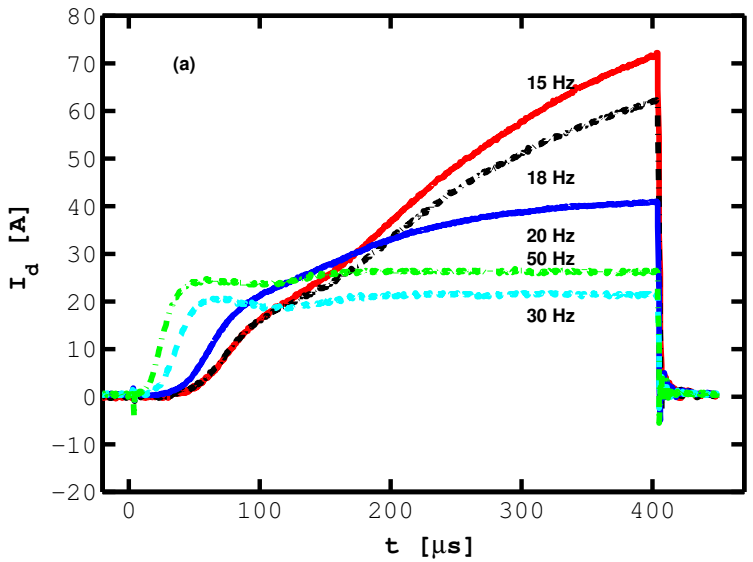

After Magnus et al. (2012), JVSTA **30** 050601

HiPIMS - Voltage - Current - time

- The observed changes in the discharge current are reflected in the flux of ions impinging on the substrate

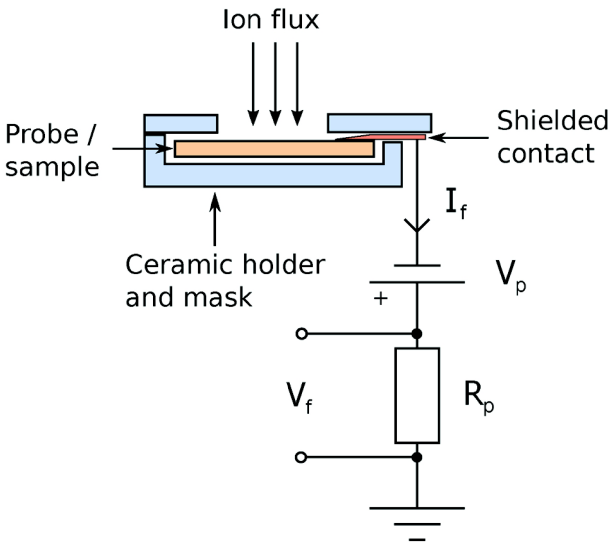

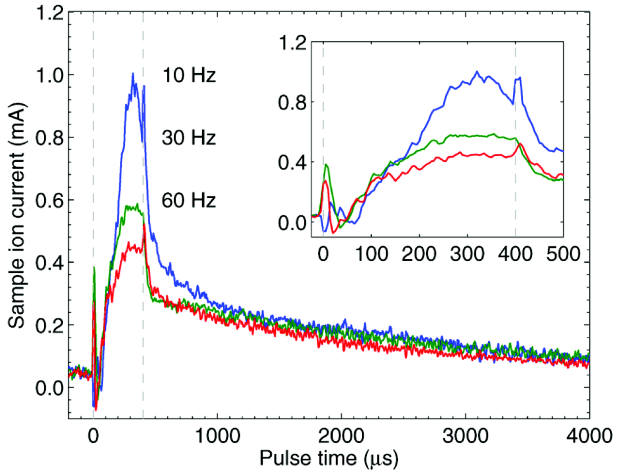

From Magnus et al. (2011), JAP **110** 083306

HiPIMS - Voltage - Current - time

- At high frequencies, nitride or oxide is not able to form between pulses, and self-sputtering by Ti^+-ions (singly and multiply charged) from a Ti target is the dominant process
- At low frequency, the long off-time results in a nitride or oxide layer being formed on the target surface and self-sputtering by Ti^+- and N^+-ions or O^+-ions from TiN or TiO_2 takes place

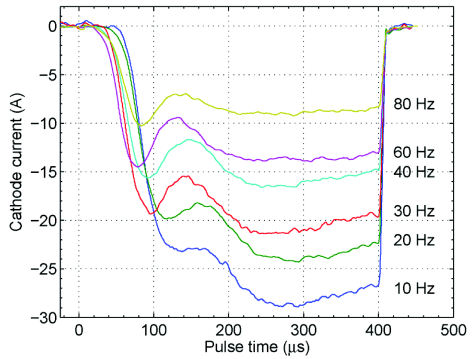

From Magnus et al. (2011), JAP **110** 083306

and Magnus et al. (2012), JVSTA **30** 050604

HiPIMS - Voltage - Current - time

- As the oxygen flow is increased a transition to oxide mode is observed

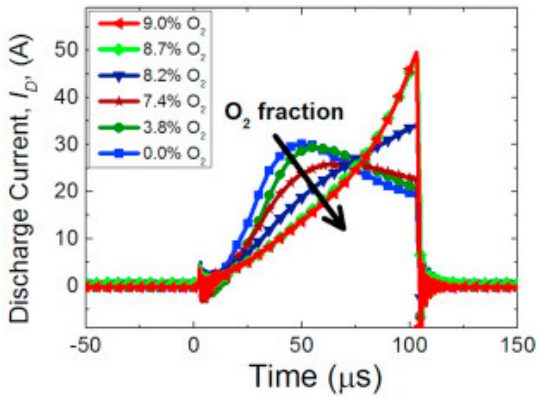

The current waveforms for an Ar/O_2 discharge with a V target where the oxygen flow rate is varied

From Aijaz et al. (2016) Solar Energy Materials and Solar Cells **149** 137

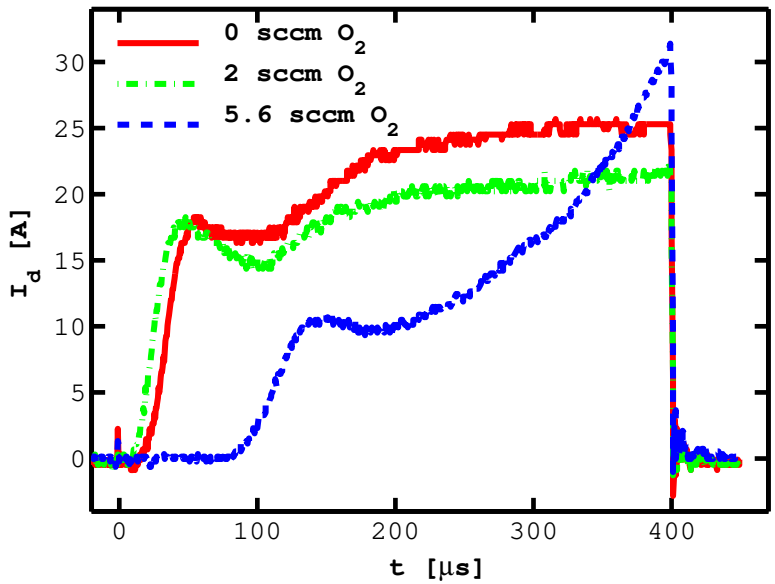

The current waveforms for an Ar/O_2 discharge with a Ti target where the oxygen flow rate is varied – 600 V, 50 Hz and 0.6 Pa

From Gudmundsson et al. (2013), ISSP 2013, p. 192

Gudmundsson (2016) Plasma Phys. Contr. Fus. **58** 014002

HiPIMS - Voltage - Current - time

- The working gas pressure is roughly 0.6 Pa and the pulse voltage is 600 V and this voltage is maintained throughout the pulse
- The discharge current decreases when 2 sccm of oxygen is added to the discharge
- It has been confirmed that in the oxide mode, the discharge is dominated by O^+-ions, due to oxygen atoms sputtered off the target surface

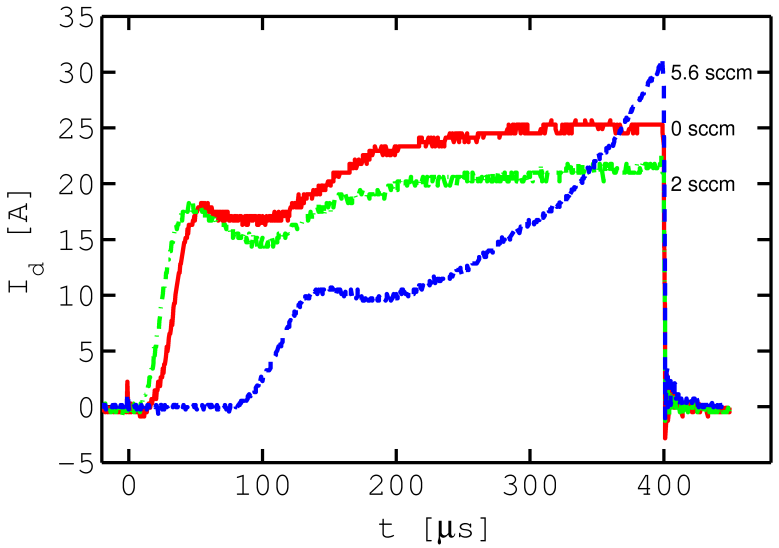

The discharge current waveforms for an Ar/O_2 discharge with a Ti target where the oxygen flow rate is varied – 600 V, 50 Hz and 0.6 Pa

From Gudmundsson et al. (2013), ISSP 2013, p. 192

HiPIMS - Voltage - Current - time

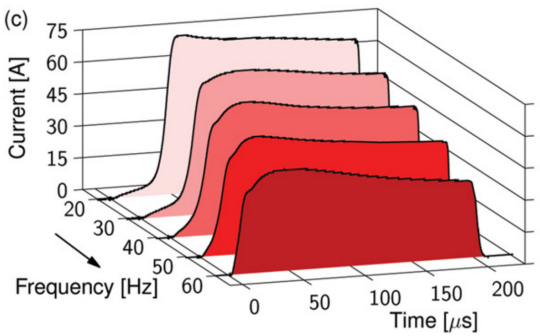

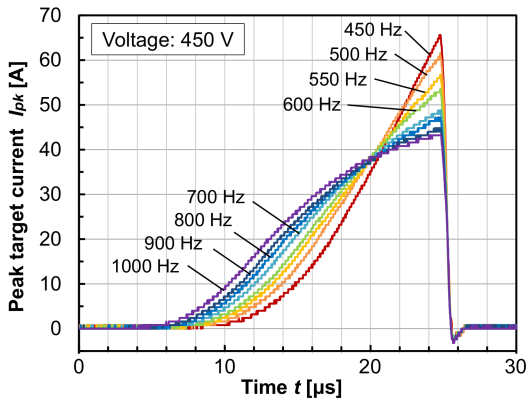

- Similar behaviour has been reported for various target and reactive gas combinations
  - The discharge current increases with decreased repetition frequency
  - The discharge current waveform maintains its shape for Ar/O_2 discharge with Nb target

    From Hála et al. (2012), JPD **45** 055204
  - The discharge current waveform becomes distinctly triangular for Ar/N_2 discharge with Hf target

    From Shimizu et al. (2015), JPD **49** 065202

HiPIMS - Voltage - Current - time

- The current increases with increased partial pressure of the reactive gas
  - The current waveform becomes distinctly triangular for Ar/N_2 discharge with Al target

    From Moreira et al. (2015), JVSTA **33** 021518
  - The current waveform maintains its shape for Ar/O_2 discharge with Nb target

    From Hála et al. (2012), JPD **45** 055204

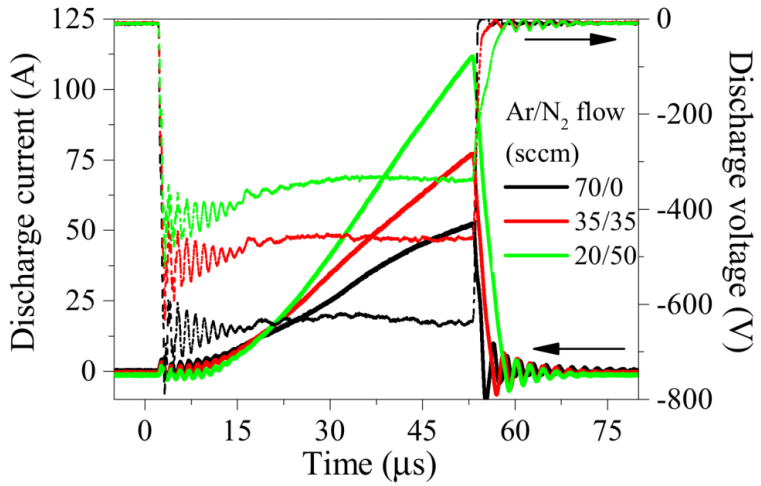

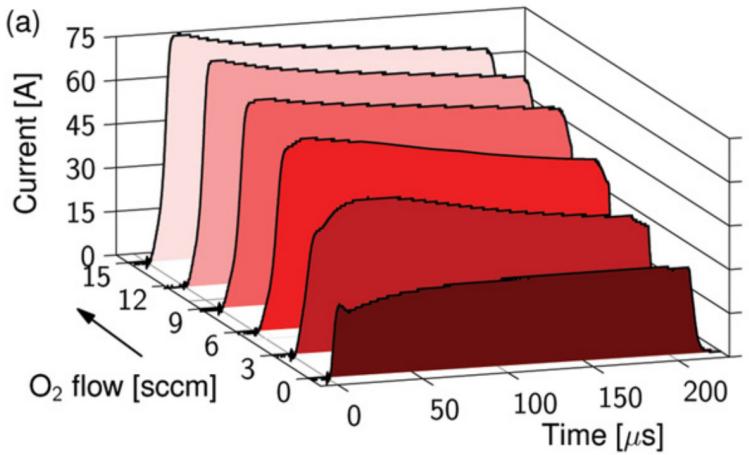

Ionization region model studies of reactive HiPIMS

Ionization region model studies of reactive HiPIMS

- The species assumed in the reactive-IRM are
  - cold electrons e^C, hot electrons e^H
  - argon atoms Ar($3s^2 3p^6$), warm argon atoms in the ground state Ar^W, hot argon atoms in the ground state Ar^H, Ar^m ($1s_5$ and $1s_3$) (11.6 eV), argon ions Ar^+ (15.76 eV)
  - titanium atoms Ti($a\,^3F$), titanium ions Ti^+ (6.83 eV), doubly ionized titanium ions Ti^{2+} (13.58 eV)
  - oxygen molecule in the ground state $O_2(X^3\Sigma_g^-)$, the metastable oxygen molecules $O_2(a^1\Delta_g)$ (0.98 eV) and $O_2(b^1\Sigma_g)$ (1.627 eV), the oxygen atom in the ground state $O(^3P)$, the metastable oxygen atom $O(^1D)$ (1.96 eV), the positive ions O_2^+ (12.61 eV) and O^+ (13.62 eV), and the negative ion O^-

Toneli et al. (2015) J. Phys. D. **48** 325202

Ionization region model studies of reactive HiPIMS

- The sputter yield for the various bombarding ions was calculated by TRIDYN for
  - **Metal mode** – Ti target
  - **Poisoned mode** – TiO_2 target
- The yields correspond to the extreme cases of either clean Ti surface and a surface completely oxidized (TiO_2 surface)
- The sputter yield is much lower for poisoned target

The sputter yield data is from Tomas Kubart, Uppsala University

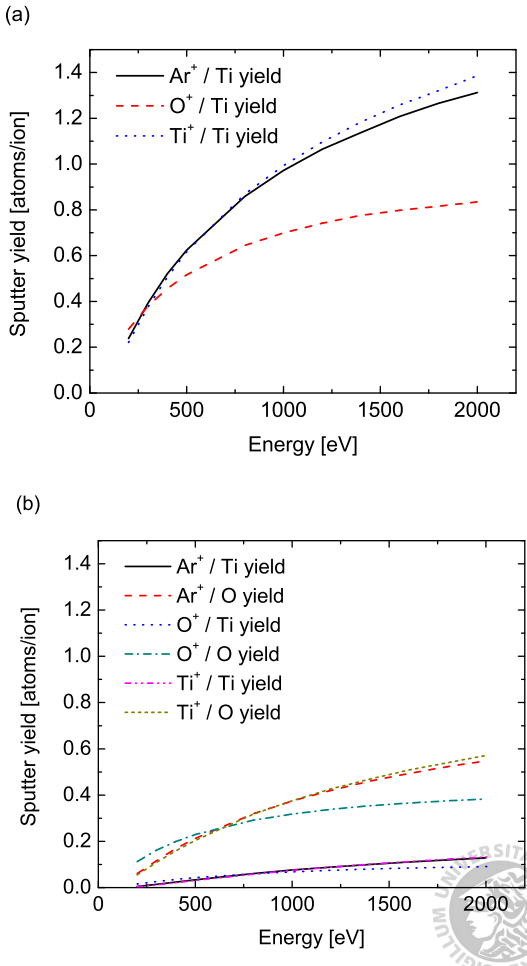

Ionization region model studies of reactive HiPIMS

- The model is applied to explore Ar/O_2 discharge with Ti target in both metal mode and oxide (poisoned) mode
- The IRM is a semi-empirical model in the sense that it uses a measured discharge voltage and current waveforms as a main input parameter
- For this study we use the measured curve for Ar/O_2 with Ti target at 50 Hz for metal mode and at 15 Hz for poisoned mode

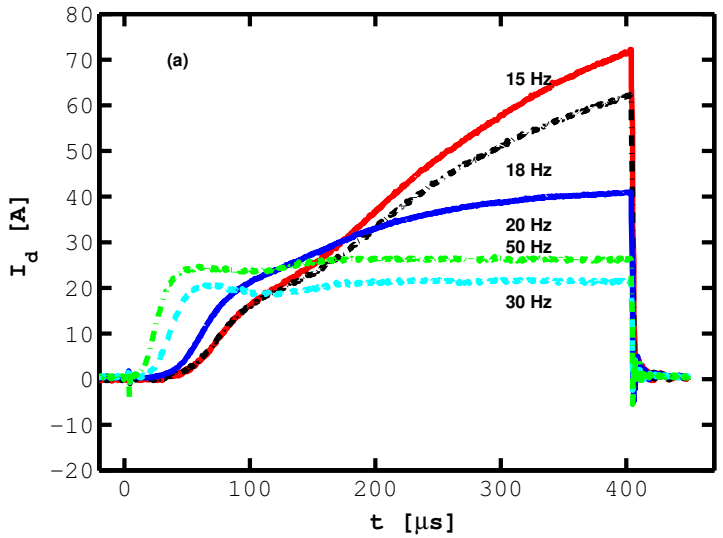

After Magnus et al. (2012), JVSTA **30** 050601

Ionization region model studies of reactive HiPIMS

- The gas rarefaction is observed for the argon atoms but is more significant for the O_2 molecule
- Due to the rarefaction the density of Ti atoms is higher than the O_2 density
- The atomic oxygen density is over one order of magnitude lower than the molecular oxygen density – the dissociation fraction is low

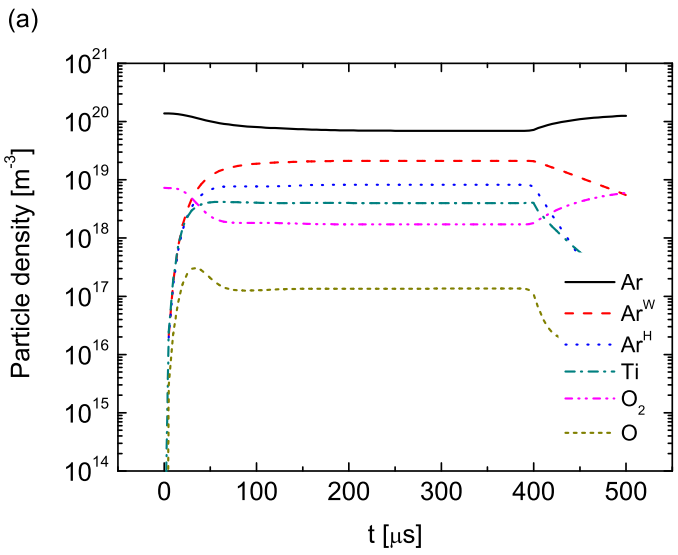

The temporal evolution of the neutral species with **5 % oxygen partial flow** rate for Ar/O_2 discharge with Ti target in **metal mode**.

Gudmundsson et al. (2016) PSST **25**(6) 065004

Ionization region model studies of reactive HiPIMS

- Gas rarefaction is observed for both argon atoms and O_2 molecules
- The density of Ti atoms is lower than both the O_2 density and atomic oxygen density
- The atomic oxygen density is higher than the O_2 density towards the end of the pulse

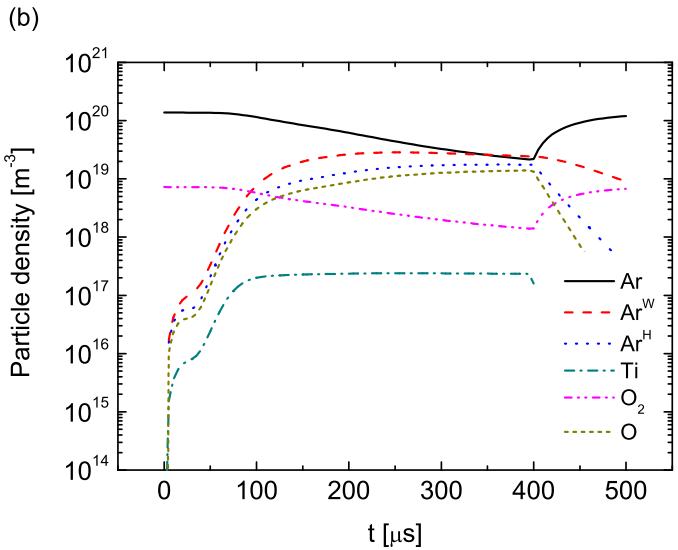

The temporal evolution of the neutral species with **5 % oxygen partial flow** rate for Ar/O_2 discharge with Ti target in **poisoned mode**.

Gudmundsson et al. (2016) PSST **25**(6) 065004

Ionization region model studies of reactive HiPIMS

- The increase in the atomic oxygen in the ground state is due to:
  - sputtering of $O(^3P)$ from the partially to fully oxidized target (dominates)
  - electron impact de-excitation of $O(^1D)$
  - electron impact dissociation of the O_2 ground state molecule

The temporal evolution of the neutral species with **5 % oxygen partial flow** rate for Ar/O_2 discharge with Ti target in **transition mode** and **poisoned mode**.

Lundin et al. (2017) JAP **121**(17) 171917

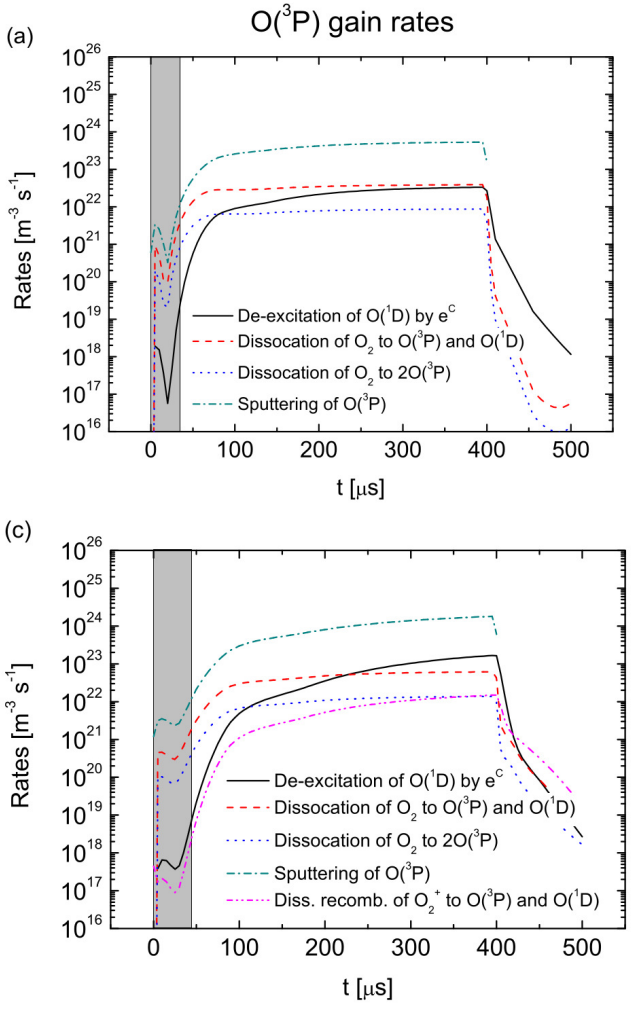

Ionization region model studies of reactive HiPIMS

- Ar^+ and Ti^+-ions dominate the discharge
- Ti^{2+}-ions follow by roughly an order of magnitude lower density
- The O_2^+ and O^+-ion density is much lower

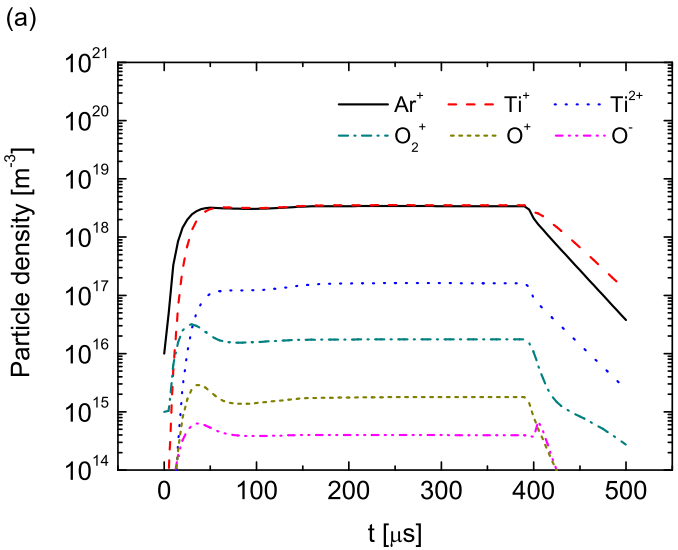

The temporal evolution of the neutral species with **5 % oxygen partial flow** rate for Ar/O_2 discharge with Ti target in **metal mode**.

Gudmundsson et al. (2016) PSST **25**(6) 065004

Ionization region model studies of reactive HiPIMS

- Ar^+-ions dominate the discharge
- Ti^+, O^+, have very similar density, but the temporal variation is different, and the O_2^+ density is slightly lower
- The Ti^{2+}-ion density increases fast with time and overcomes the O_2^+ density towards the end of the pulse

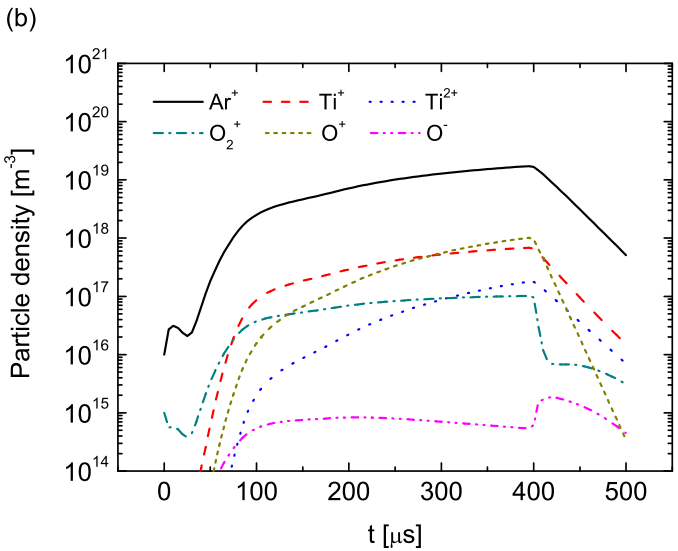

The temporal evolution of the neutral species with **5 % oxygen partial flow** rate for Ar/O_2 discharge with Ti target in **poisoned mode**.

Gudmundsson et al. (2016) PSST **25**(6) 065004

Ionization region model studies of reactive HiPIMS

- Ar^+ and Ti^+-ions contribute most significantly to the discharge current at the cathode target surface – almost equal contribution

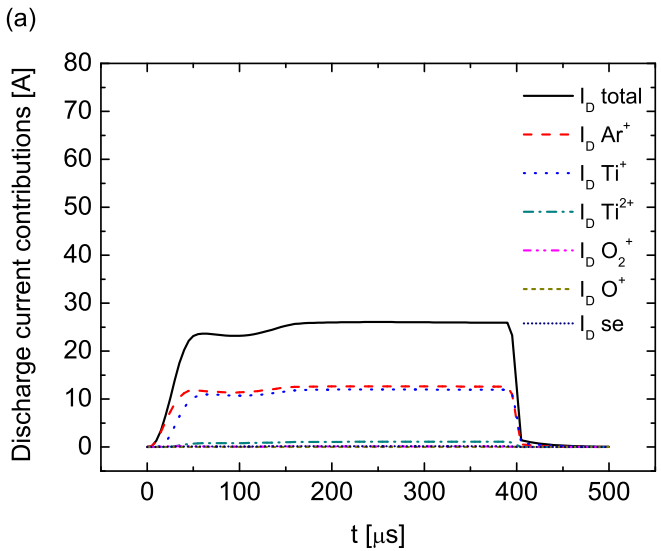

The temporal evolution of the neutral species with **5 % oxygen partial flow** rate for Ar/O_2 discharge with Ti target in **metal mode**.

Gudmundsson et al. (2016) PSST **25**(6) 065004

Ionization region model studies of reactive HiPIMS

- Ar^+ contribute most significantly to the discharge current – almost solely – at the cathode target surface
- The contribution of secondary electron emission is very small

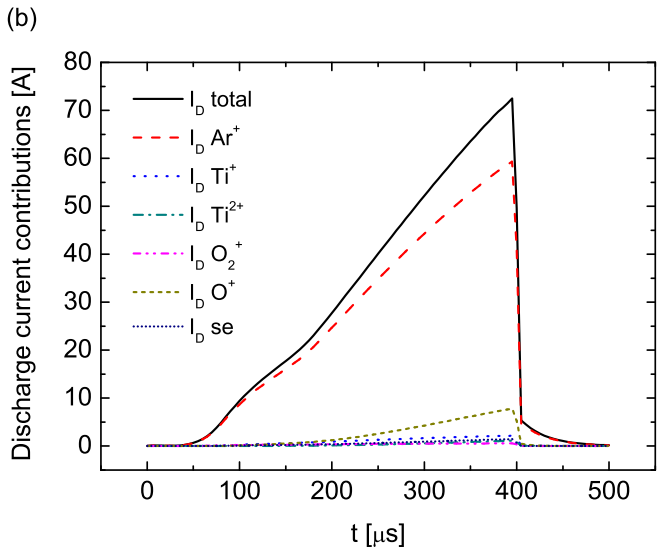

The temporal evolution of the neutral species with **5 % oxygen partial flow** rate for Ar/O_2 discharge with Ti target in **poisoned mode**.

Gudmundsson et al. (2016) PSST **25**(6) 065004

Ionization region model studies of reactive HiPIMS

- Recycling of atoms coming from the target and then ionized are required for the current generation in both modes of operation
- In the metal mode self-sputter recycling dominates and in the poisoned mode working gas recycling dominates
- The dominating type of recycling determines the discharge current waveform

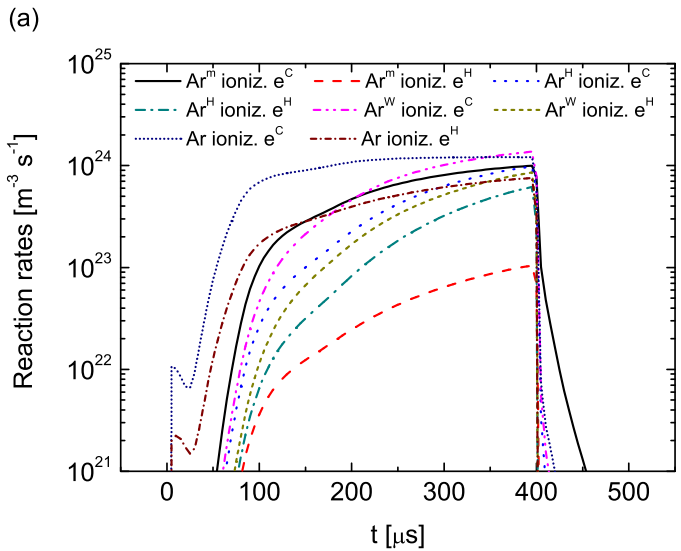

The temporal variations of the reaction rates for electron impact ionization of the argon atoms (ground state plus metastable) in poisoned mode.

Gudmundsson et al. (2016) PSST **25**(6) 065004

Ionization region model studies of reactive HiPIMS

- The temporal variations of the reaction rates for electron impact ionization of the argon atoms (ground state plus metastable)
- The individual rates for all the reactions in the poisoned mode
- The sum of the ionization rates for the e^C plus the e^H populations, and that for the e^H electron population alone

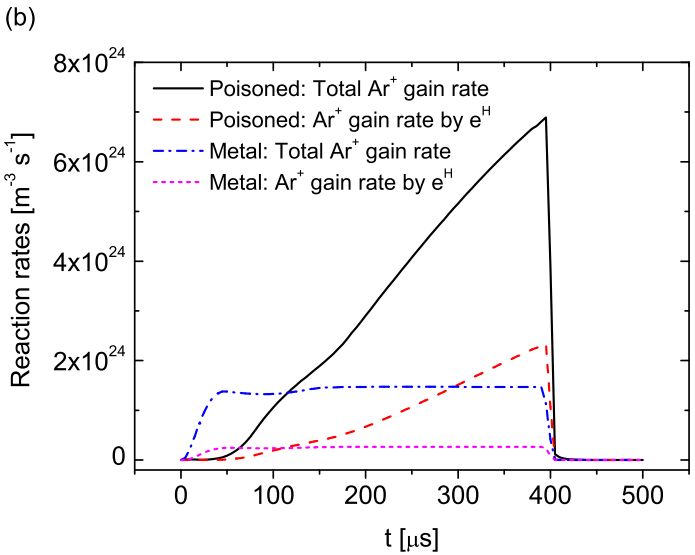

The temporal variations of the reaction rates for the creation of Ar^+ ions.

Gudmundsson et al. (2016) PSST **25**(6) 065004

Ionization region model studies of reactive HiPIMS

- The O_2 ground state molecule density is strongly reduced during the discharge pulse in all modes of operation
- In the metal mode, it is reduced by 67 % during the current plateau at around 300 μs, in the transition mode by 71 % and in the poisoned mode 80 % at the peak discharge current
- At about 200 μs into the pulse in the poisoned mode, the O(^{3}P) becomes more abundant than the O_2 ground state molecule

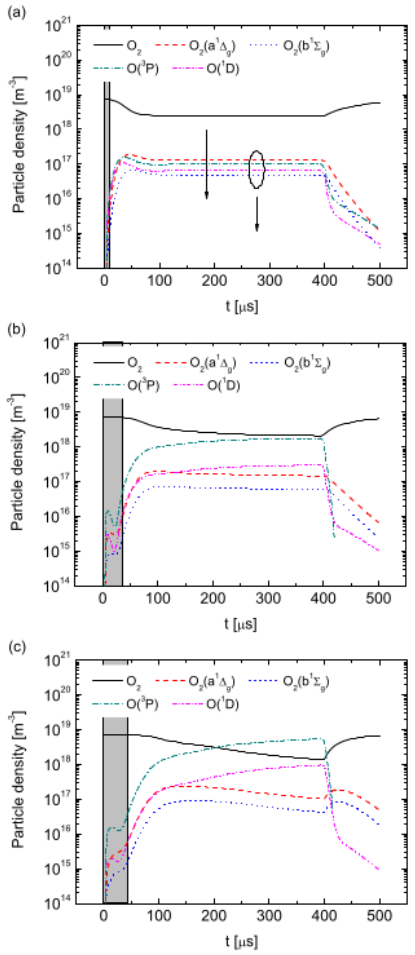

Ionization region model studies of reactive HiPIMS

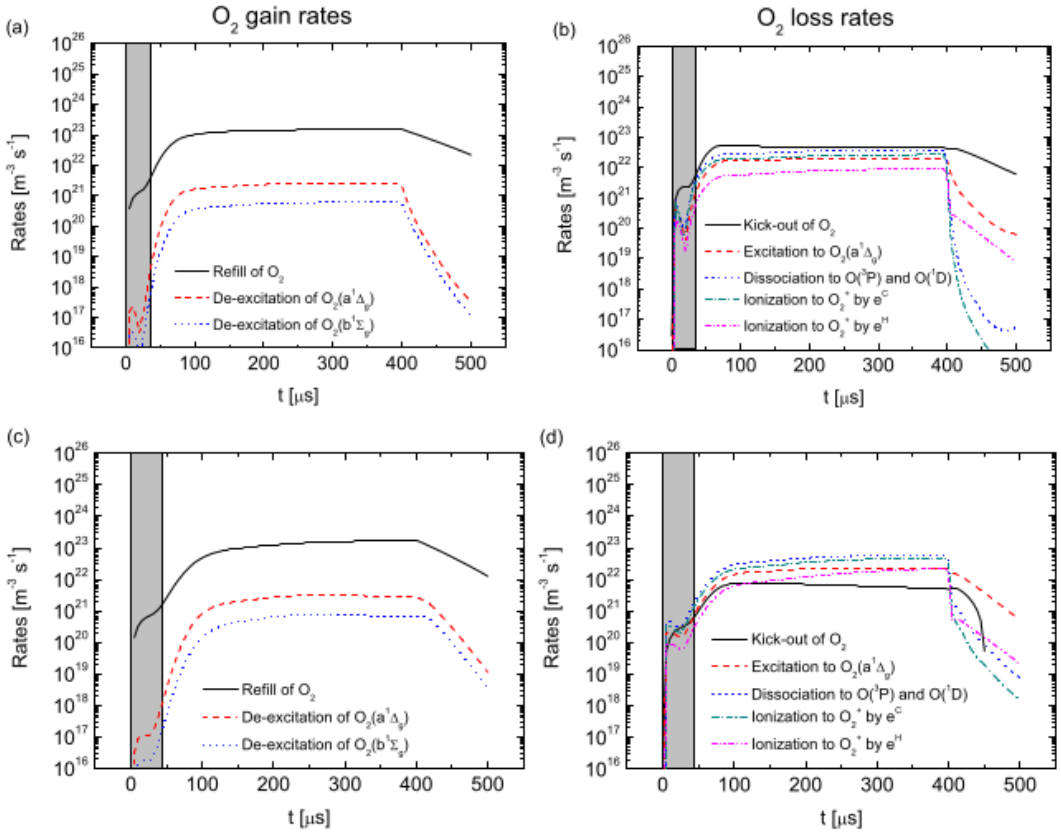

Lundin et al. (2017), JAP **121**(17) 171917

The temporal variations of the most important reaction rates for gain and loss of O_2 ground state molecules in (a-b) **transition mode** and (c-d) **poisoned mode** in with **5 % oxygen partial flow rate** for Ar/O_2 discharge with Ti target.

Ionization region model studies of reactive HiPIMS

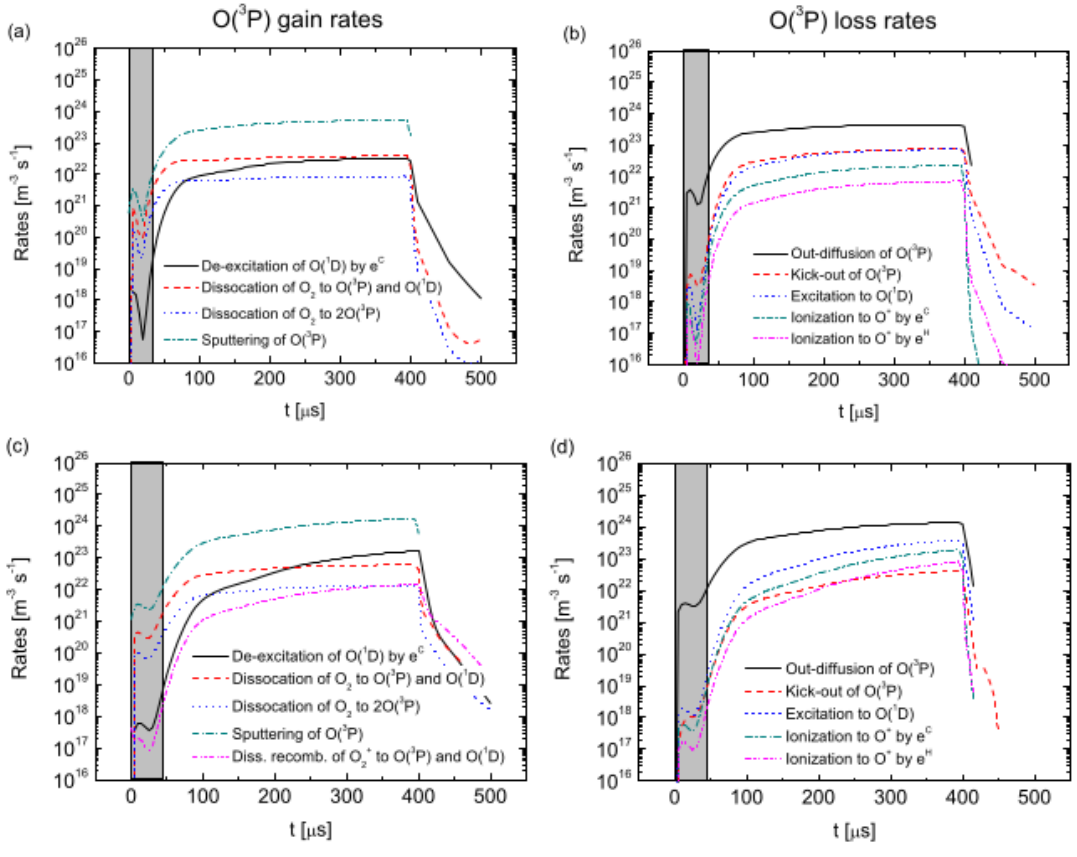

Lundin et al. (2017), JAP **121**(17) 171917

The temporal variations of the most important reaction rates for gain and loss of O(^{3}P) ground state atom in (a-b) **transition mode** and (c-d) **poisoned mode** in with **5 % oxygen partial flow rate** for Ar/O_2 discharge with Ti target.

Ionization region model studies of reactive HiPIMS

- The temporal variation of the density of Ti neutrals and ions as well as atomic oxygen neutrals and positive ions
- The Ti ionization fraction increases as we transition from metal mode into poisoned mode
- The ionized flux fraction for Ti towards the end of the pulse is 35 % in metal mode, 49 % in the transition mode, and 64 % in the poisoned mode

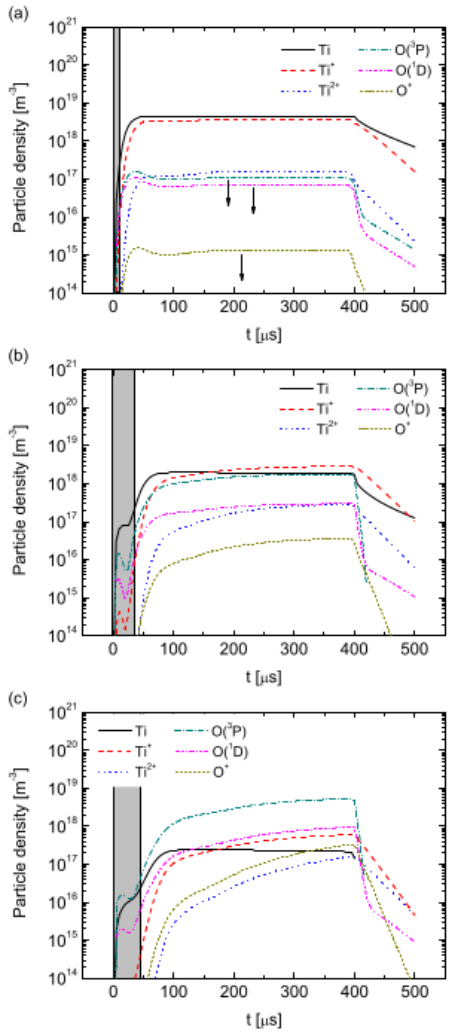

Lundin et al. (2017), JAP **121**(17) 171917

Ionization region model studies of reactive HiPIMS

- The transition to continuously increasing triangular-shaped has been observed experimentally for a Cr target operated in an Ar/O_2 mixture
- Using *in situ* spatially resolved XPS the surface composition of the Cr target was recorded
- Only when the target race track was completely covered by an oxide layer, the triangular pulse shape is observed
- In all other cases, a plateau current was observed

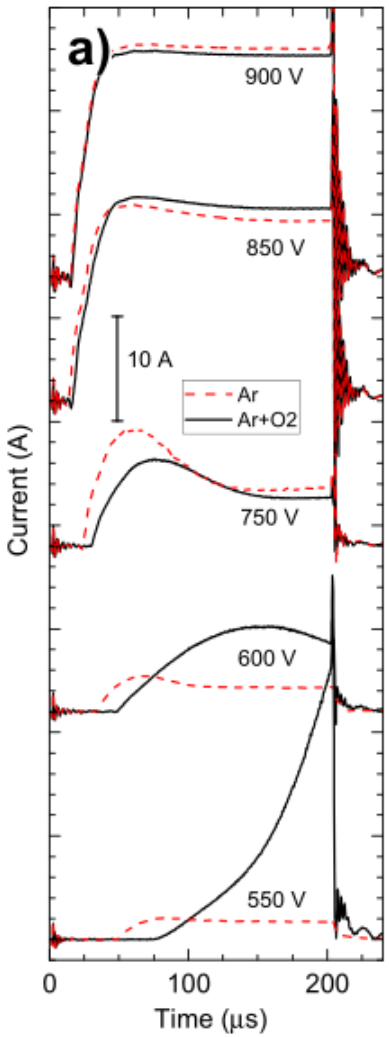

Layes et al. (2018) PSST **27**(8) 084004

Ionization region model studies of reactive HiPIMS

- If at least 20% of the target area is metallic, then metal atom recycling dominates and a plateau current is observed
- Discharge current waveforms for different applied voltages at discharge frequency of 20 Hz, without and with 0.4% O_2 in the gas mixture
- The profiles of the atomic metal fraction (at%) along the radius of the targets

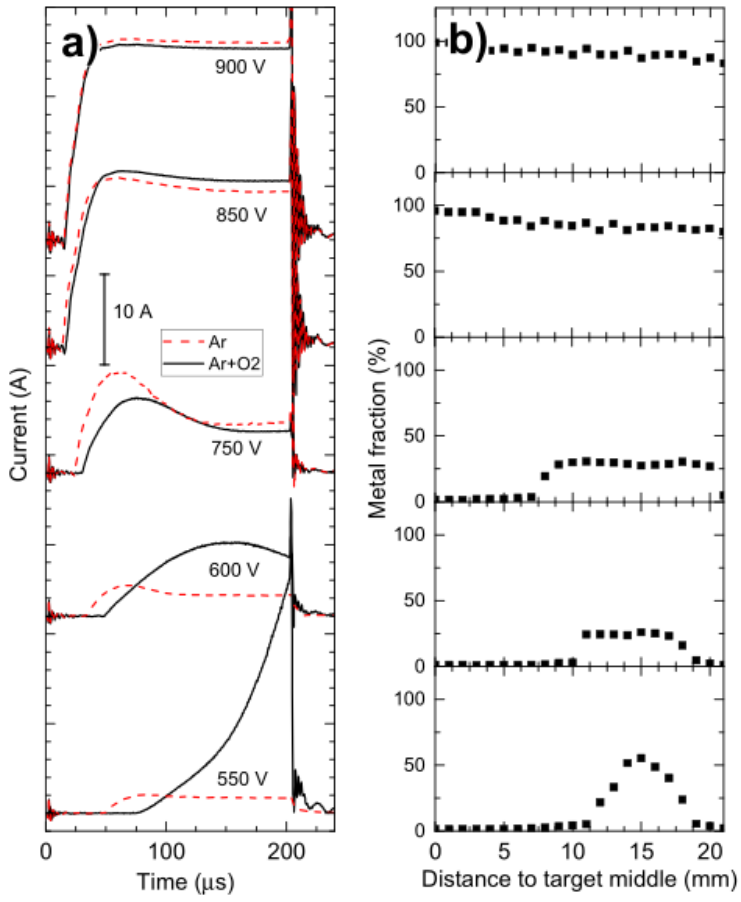

Layes et al. (2018) PSST **27**(8) 084004

Ionization region model studies of reactive HiPIMS

- In the metal mode sheath energization was found to be only 10 %
  - same range as the results reported earlier for an Al target

    Huo et al. (2013), PSST **22**(4) (2013) 045005

  the dominating electron heating mechanism is Ohmic heating
- For the poisoned mode the sheath energization was 30 %, with a rising trend, at the end of the pulse
- This is due to the secondary electron emission
  - In the poisoned mode essentially all the ions (mainly Ar^+, but also O^+ and Ti^{2+} towards the end of the pulse) contribute to the secondary electron emission
  - In the metal mode only half of the ions contribute to the secondary electron emission (Ar^+) while the other half does not contribute at all ($\gamma_{Ti^+} = 0.0$)

The generalized recycling model

Generalized recycling

- The total current carried by working gas ions

$$I_g = I_{prim} + I_{gas-recycle} = I_{prim}\left(1 + \frac{\pi_g}{1-\pi_g}\right)$$

- A working gas-sputtering parameter

$$\pi_g = \alpha_g \beta_g \xi_{pulse}$$

where

  - α_g is ionization probability
  - β_g is back attraction probability
  - $\xi_{pulse} = 1$ is return fraction in a pulse

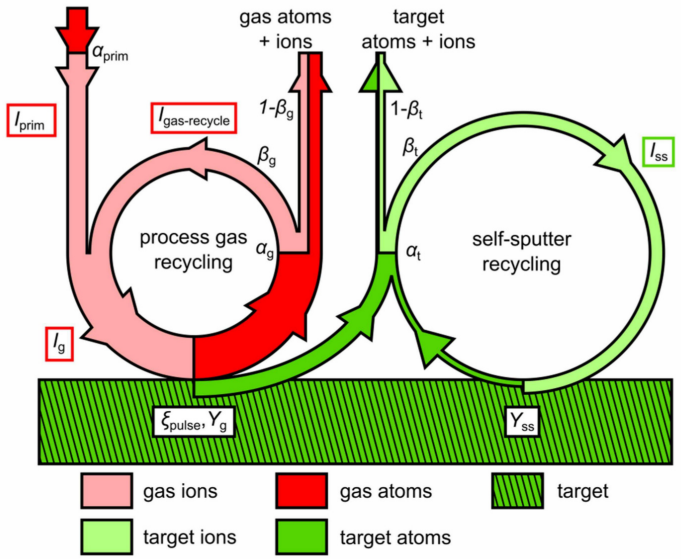

From Brenning et al. (2017) PSST **26** 125003

Generalized recycling

- The total self-sputter current is

$$I_{SS} = I_g \left(\frac{Y_g}{Y_{SS}} \frac{\pi_{SS}}{1 - \pi_{SS}} \right)$$

where the self-sputter parameter is

$$\pi_{SS} = \alpha_t \beta_t Y_{SS}$$

- The total discharge current is

$$I_D = I_{prim} + I_{gas-recycle} + I_{SS}$$

$$= I_{prim} \left(1 + \frac{\pi_g}{1 - \pi_g} \right) \left(1 + \frac{Y_g}{Y_{SS}} \frac{\pi_{SS}}{1 - \pi_{SS}} \right)$$

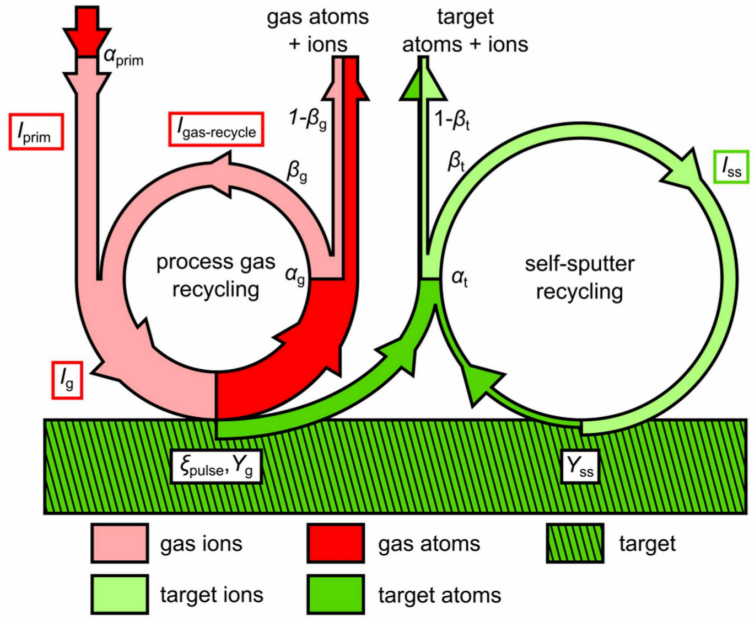

From Brenning et al. (2017) PSST **26** 125003.

Generalized recycling

- The discharge current

$$I_{\mathrm{D}} = I_{\mathrm{prim}} \Pi_{\mathrm{gas-recycle}} \Pi_{\mathrm{SS-recycle}}$$

- I_{prim} is the seed current that acts as a seed to the whole discharge current and has an upper limit I_{crit}
- $I_{\mathrm{prim}} \Pi_{\mathrm{gas-recycle}}$ is the seed current for the self-sputter process
- If $\pi_{\mathrm{SS}} > 1$ the discharge goes into SS-runaway

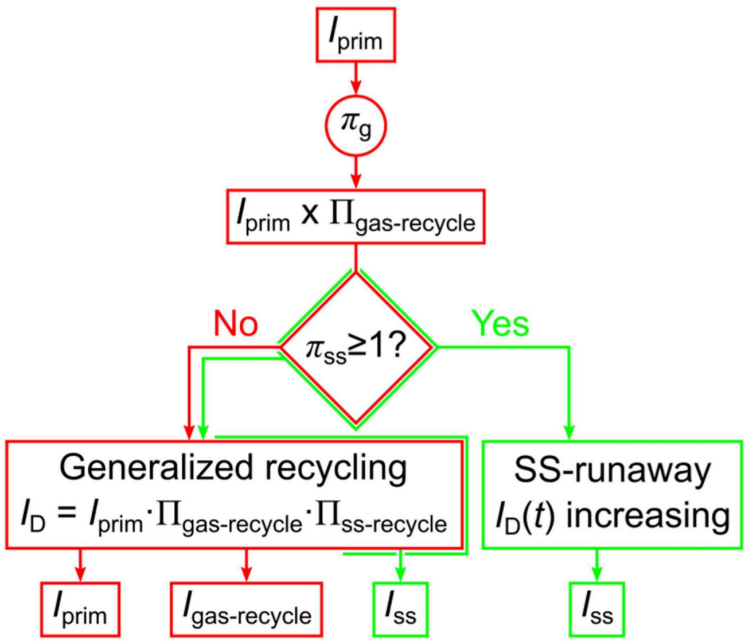

From Brenning et al. (2017) PSST **26** 125003

Generalized recycling

- Recycling map
- A graph in which the ion current mix of I_{prim}, $I_{\mathrm{gas-recycle}}$, and I_{SS} to the target in a magnetron discharge is defined by a point
- The value of $I_{\mathrm{prim}}/I_{\mathrm{D}} = 39$ %, can be read on the diagonal lines ($Y_{\mathrm{SS}} = 0.5$)
- $I_{\mathrm{prim}}/I_{\mathrm{D}} \geq 0.85$ defines the dcMS regime
- For $I_{\mathrm{SS}}/I_{\mathrm{D}} > 0.5$ we have the SS-recycle dominated range A
- For $I_{\mathrm{gas-recycle}}/I_{\mathrm{D}} > 0.5$ we have the gas-recycle dominated range B

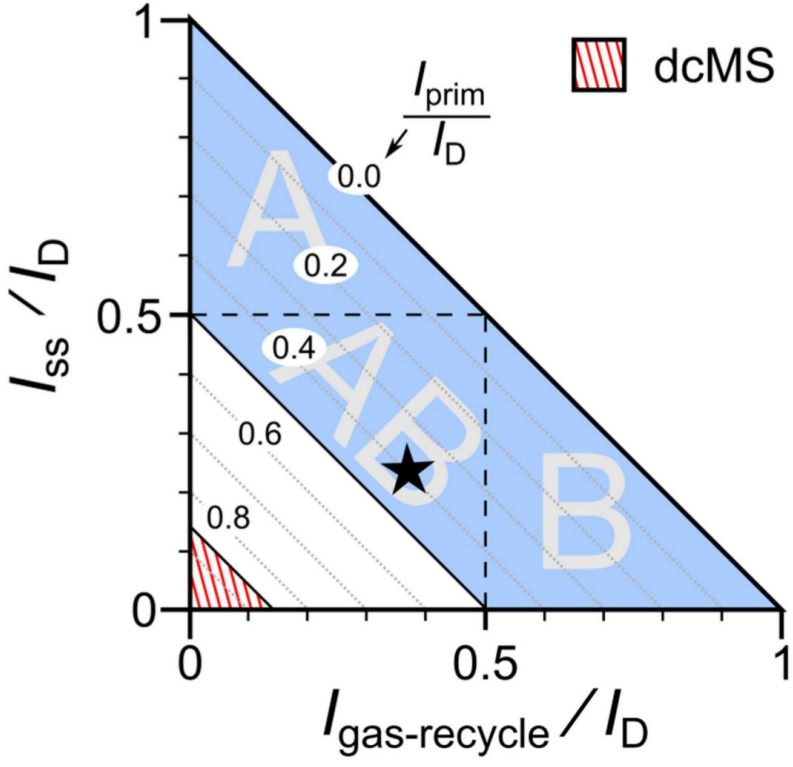

From Brenning et al. (2017) PSST **26** 125013

Generalized recycling

- The discharge with Al target moves from the dcMS regime to the HiPIMS discharge regime with increased discharge voltage – **type A**
- A discharge with carbon target jumps from the dcMS regime to the HiPIMS regime – both SS recycling and working gas recycling play a role – intermediate **type AB**

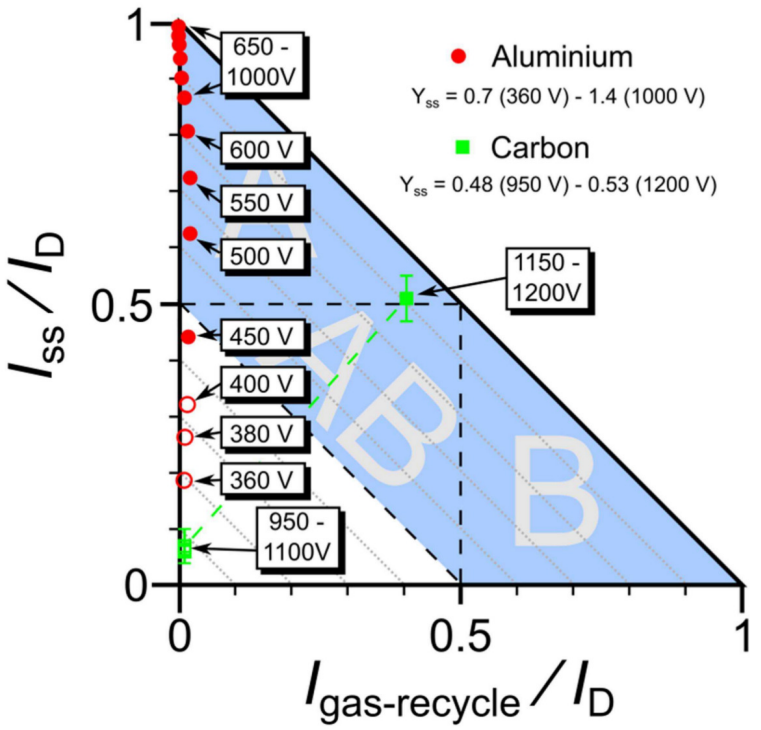

From Brenning et al. (2017) PSST **26** 125003

Generalized recycling

- Recycling map for five different targets with varying self-sputter yield
  - Cu – $Y_{SS} = 2.6$
  - Al – $Y_{SS} = 1.1$
  - Ti – $Y_{SS} = 0.7$
  - C – $Y_{SS} = 0.5$
  - TiO_2 – $Y_{SS} = 0.04 - 0.25$
- For very high self-sputter yields $Y_{SS} > 1$, the discharges above I_{crit} are of **type A** with dominating **SS-recycling**
- For very low self-sputter yields $Y_{SS} < 0.2$, the discharges above I_{crit} are of **type B** with dominating **working gas recycling**

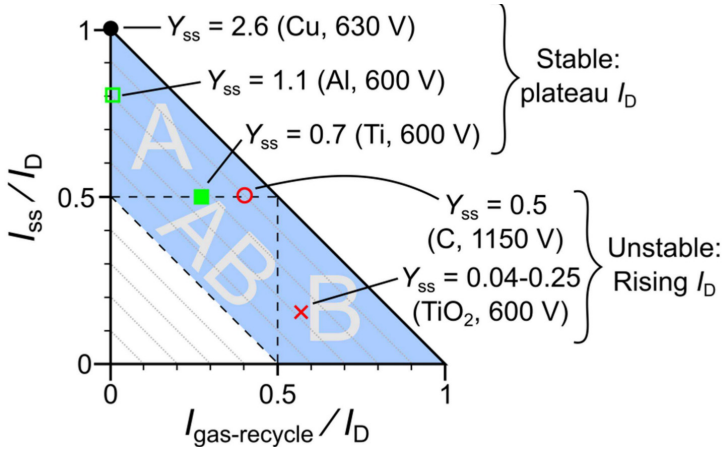

From Brenning et al. (2017), PSST **26** 125003

Generalized recycling

- Recycling loops
- Discharge with Al target – SS recycling dominates
  - high self sputter yield
- Reactive discharge with TiO_2 target – working gas recycling dominates
  - low self sputter yield

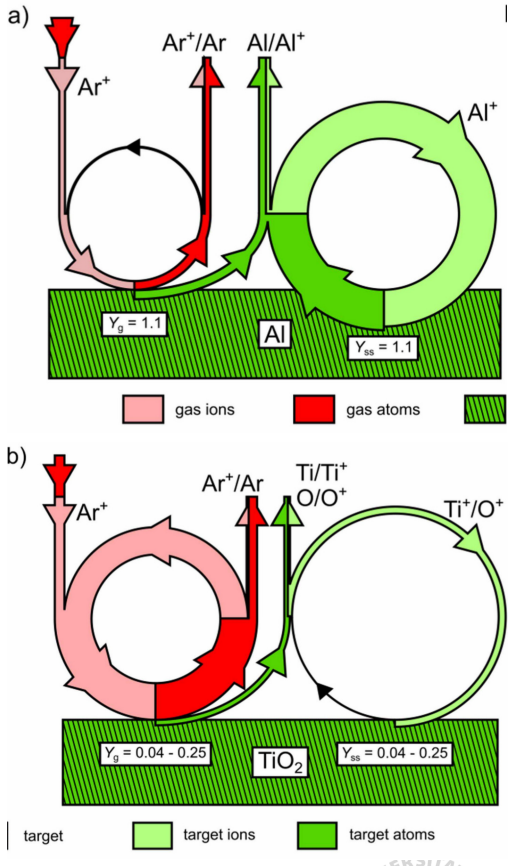

From Brenning et al. (2017) PSST **26** 125003

HiPIMS - Voltage - Current - time

- For Ar/O_2 discharge with Ti target
- At high frequencies, oxide is not able to form between pulses, and **self-sputtering recycling** by Ti^+-ions is the dominant process
- At low frequency, the long off-time results in an oxide layer being formed (TiO_2) on the target surface and **working gas recycling dominates** – triangular current waveform

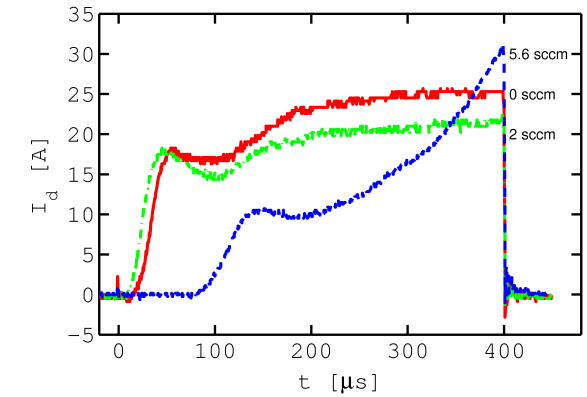

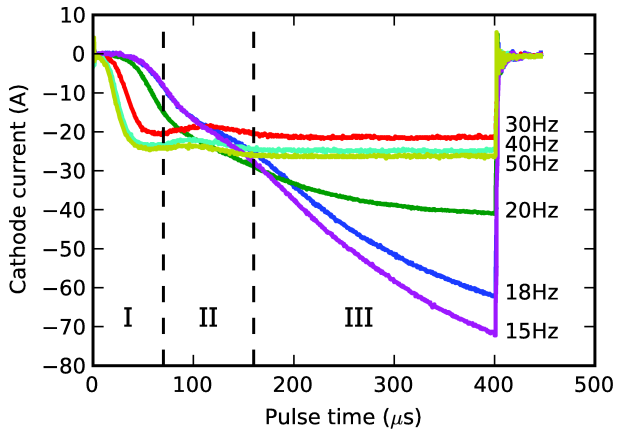

From Gudmundsson (2016) PPCF **58** 014002

Magnus et al. (2012) JVSTA **30** 050601

Ion energy and composition

HiPIMS - Ion energy and composition

- For non-reactive HiPIMS the IEDs show
  - the metal ions – an intense high energy tail extending to the limit of the measurement equipment
  - the ions of the working gas exhibit much lower energy
- For comparison the IEDs from dcMS show a peak at an ion energy of about 2 eV and a high-energy tail that extends to around 20 and 40 eV for Ar^+ and Ti^+, respectively

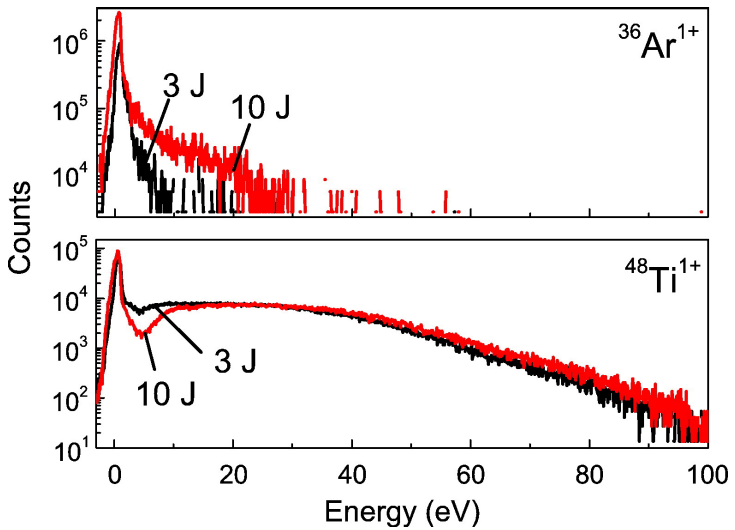

Bohlmark et al. (2006) TSF **515** 1522

HiPIMS - Ion energy and composition

- Reactive Ar/N_2 sputtering of a Cr target
- The Cr^+ ions comprise an intense low energy peak and pronounced high energy tails
- For reactive sputtering in Ar/N_2 discharges, low energy N_2^+-ions and energetic N^+-ions are present in the reactive mode
- The IED for the N^+-ion possesses a high energy tail just like the Cr^+-ions (or the Cr^{2+} ions), which is not observed for Ar^+ or N_2^+

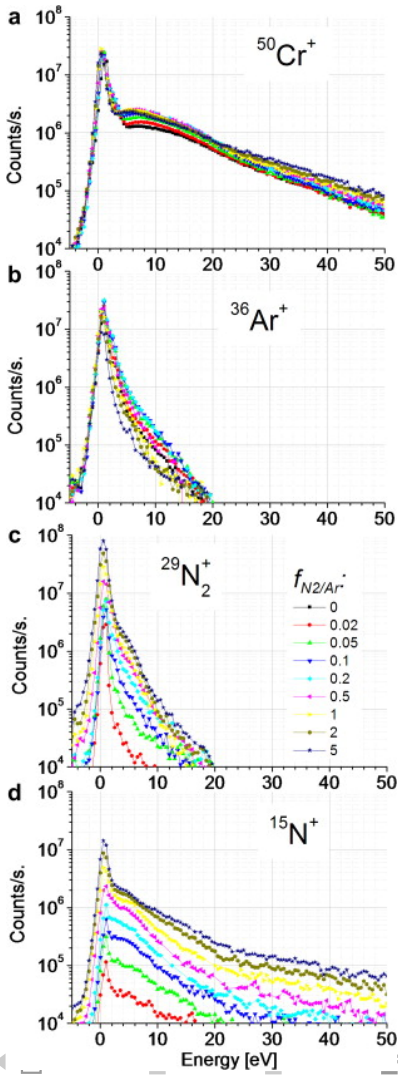

Greczynski and Hultman (2010) Vacuum **84** 1159

HiPIMS - Ion energy and composition

- Similar findings have been reported
  - Ar/N_2 discharge with Ti target – N^+ behaves like Ti^+

    (Lattemann et al., 2010; Ehiasarian et al., 2007)
  - Ar/N_2 discharge with Al target – N^+ behaves like Al^+

    (Jouan et al., 2010)
- The working gas ions and the molecular ion of the reactive gas present a similar IED
- The metal ion and the atomic ion of the reactive gas present similar IED and extend to very high energy

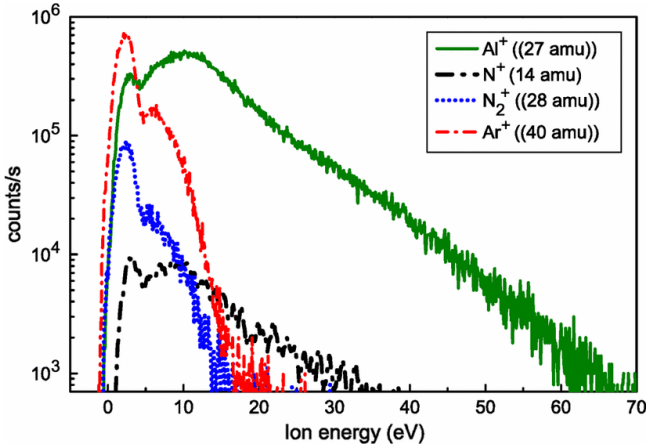

Jouan et al. (2010) IEEE TPS **38** 3089

HiPIMS - Ion energy and composition

- The time-averaged ion energy distributions (IED) of the ions in the metal and oxide modes of and Ar/O_2 discharge with Al target
- There is no difference for the distributions of Ar^+-ions between the metal and oxide modes
- There is a considerable amount of O^+-ions

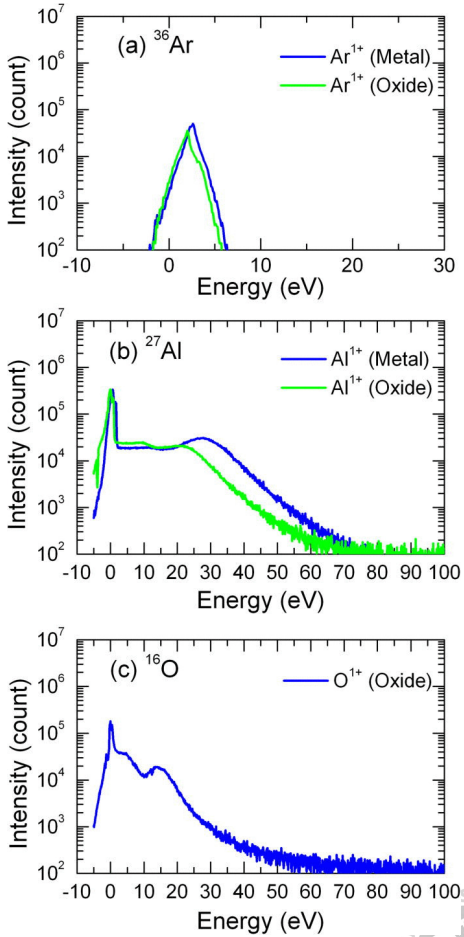

Aiempanakit et al. (2013) JAP **113** 133302

Summary

Summary

- The current-voltage-time waveforms in a reactive discharge exhibit similar general characteristics as the non-reactive case in some cases
  - the current rises to a peak, then decays because of rarefaction before rising to a self-sputtering dominated phase
  - in other cases the current develops a triangular shape as repetition frequency is lowered or the partial pressure of the reactive gas is increased
- The secondary electron emission yield is higher for a nitride or oxide target than a titanium target when self-sputtering is the dominant sputtering mechanism

Summary

- An ionization region model was used to explore the plasma composition during the high power pulse
- Comparison was made between the metal mode and the poisoned mode
  - In metal mode Ar^+ and Ti^+-ions dominate the discharge and are of the same order of magnitude
  - In poisoned mode Ar^+-ions dominate the discharge and two orders of magnitude lower, Ti^+, O^+, have very similar density, with the O_2^+ density slightly lower
  - In the metal mode Ar^+ and Ti^+-ions contribute most significantly to the discharge current while in poisoned mode Ar^+ dominate
- In the metal mode self-sputter recycling dominates and in the poisoned mode working gas recycling dominates – the dominating type of recycling determines the discharge current waveform

Thank you for your attention

The slides can be downloaded at

`http://langmuir.raunvis.hi.is/~tumi/ranns.html`

- The work is in collaboration with
  - Dr. Daniel Lundin, Linköping University, Linköping, Sweden
  - Prof. Nils Brenning, KTH Royal Institite of Technology, Stockholm, Sweden
  - Dr. Michael A. Raadu, KTH Royal Institite of Technology, Stockholm, Sweden
  - Prof. Tiberu Minea, Université Paris-Sud, Orsay, France
- We got help with the sputtering yields from
  - Dr. Tomas Kubart, Uppsala University, Uppsala, Sweden

References

Agnarsson, B., F. Magnus, T. K. Tryggvason, A. S. Ingason, K. Leosson, S. Olafsson, and J. T. Gudmundsson (2013). Rutile TiO_2 thin films grown by reactive high power impulse magnetron sputtering. *Thin Solid Films 545*, 445–450.

Aiempanakit, M., A. Aijaz, D. Lundin, U. Helmersson, and T. Kubart (2013). Understanding the discharge current behavior in reactive high power impulse magnetron sputtering of oxides. *Journal of Applied Physics 113*(13), 133302.

Aijaz, A., Y.-X. Ji, J. Montero, G. A. Niklasson, C. G. Granqvist, and T. Kubart (2016). Low-temperature synthesis of thermochromic vanadium dioxide thin films by reactive high power impulse magnetron sputtering. *Solar Energy Materials and Solar Cells 149*, 137–144.

Anders, A., J. Andersson, and A. Ehiasarian (2007). High power impulse magnetron sputtering: Current-voltage-time characteristics indicate the onset of sustained self-sputtering. *Journal of Applied Physics 102*(11), 113303.

Audronis, M. and V. Bellido-Gonzalez (2010). Hysteresis behaviour of reactive high power impulse magnetron sputtering. *Thin Solid Films 518*(8), 1962 – 1965.

Audronis, M., V. Bellido-Gonzalez, and B. Daniel (2010). Control of reactive high power impulse magnetron sputtering processes. *Surface and Coatings Technology 204*(14), 2159–2164.

Barynova, K., S. Suresh Babu, M. Rudolph, J. Fischer, D. Lundin, M. A. Raadu, N. Brenning, and J. T. Gudmundsson (2024). On working gas rarefaction in high power impulse magnetron sputtering. *Plasma Sources Science and Technology 33*(6), 065010.

Bohlmark, J., M. Lattemann, J. T. Gudmundsson, A. P. Ehiasarian, Y. A. Gonzalvo, N. Brenning, and U. Helmersson (2006). The ion energy distributions and ion flux composition from a high power impulse magnetron sputtering discharge. *Thin Solid Films 515*(5), 1522–1526.

Bradley, J. W., A. Mishra, and P. J. Kelly (2015). The effect of changing the magnetic field strength on HiPIMS deposition rates. *Journal of Physics D: Applied Physics 48*(21), 215202.

Brenning, N., J. T. Gudmundsson, M. A. Raadu, T. J. Petty, T. Minea, and D. Lundin (2017). A unified treatment of self-sputtering, process gas recycling, and runaway for high power impulse sputtering magnetrons. *Plasma Sources Science and Technology 26*(12), 125003.

Ehiasarian, A. P., Y. A. Gonzalvo, and T. D. Whitmore (2007). Time-resolved ionisation studies of the high power impulse magnetron discharge in mixed argon and nitrogen atmosphere. *Plasma Processes and Polymers 4*(S1), S309–S313.

References

Greczynski, G. and L. Hultman (2010). Time and energy resolved ion mass spectroscopy studies of the ion flux during high power pulsed magnetron sputtering of Cr in Ar and Ar/N_2 atmospheres. *Vacuum 84*(9), 1159 – 1170.

Gudmundsson, J. T. (2008). Ionized physical vapor deposition (IPVD): Magnetron sputtering discharges. *Journal of Physics: Conference Series 100*, 082002.

Gudmundsson, J. T. (2016). On reactive high power impulse magnetron sputtering. *Plasma Physics and Controlled Fusion 58*(1), 014002.

Gudmundsson, J. T., N. Brenning, D. Lundin, and U. Helmersson (2012). The high power impulse magnetron sputtering discharge. *Journal of Vacuum Science and Technology A 30*(3), 030801.

Gudmundsson, J. T., D. Lundin, N. Brenning, M. A. Raadu, C. Huo, and T. M. Minea (2016). An ionization region model of the reactive Ar/O_2 high power impulse magnetron sputtering discharge. *Plasma Sources Science and Technology 25*(6), 065004.

Gudmundsson, J. T., F. Magnus, T. K. Tryggvason, S. Shayestehaminzadeh, O. B. Sveinsson, and S. Olafsson (2013). Reactive high power impulse magnetron sputtering. In *Proceedings of the XII International Symposium on Sputtering and Plasma Processes (ISSP 2013)*, pp. 192–194.

Hajihoseini, H. and J. T. Gudmundsson (2017). Vanadium and vanadium nitride thin films grown by high power impulse magnetron sputtering. *Journal of Physics D: Applied Physics 50*(50), 505302.

Hála, M., J. Čapek, O. Zabeida, J. E. Klemberg-Sapieha, and L. Martinu (2012). Hysteresis - free deposition of niobium oxide films by HiPIMS using different pulse management strategies. *Journal of Physics D: Applied Physics 45*(5), 055204.

Helmersson, U., M. Lattemann, J. Bohlmark, A. P. Ehiasarian, and J. T. Gudmundsson (2006). Ionized physical vapor deposition (IPVD): A review of technology and applications. *Thin Solid Films 513*(1-2), 1–24.

Huo, C., D. Lundin, J. T. Gudmundsson, M. A. Raadu, J. W. Bradley, and N. Brenning (2017). Particle-balance models for pulsed sputtering magnetrons. *Journal of Physics D: Applied Physics 50*(35), 354003.

Huo, C., D. Lundin, M. A. Raadu, A. Anders, J. T. Gudmundsson, and N. Brenning (2013). On sheath energization and ohmic heating in sputtering magnetrons. *Plasma Sources Science and Technology 22*(4), 045005.

Huo, C., M. A. Raadu, D. Lundin, J. T. Gudmundsson, A. Anders, and N. Brenning (2012). Gas rarefaction and the time evolution of long high-power impulse magnetron sputtering pulses. *Plasma Sources Science and Technology 21*(4), 045004.

References

Jouan, P.-Y., L. Le Brizoual, C. Cardinaud, S. Tricot, and M. A. Djouadi (2010). HiPIMS ion energy distribution measurements in reactive mode. *IEEE Transactions on Plasma Science 38*(11), 3089–3094.

Kubart, T., M. Aiempanakit, J. Andersson, T. Nyberg, S. Berg, and U. Helmersson (2011). Studies of hysteresis effect in reactive HiPIMS deposition of oxides. *Surface and Coatings Technology 205*(Supplement 2), S303–S306.

Lattemann, M., U. Helmersson, and J. E. Greene (2010). Fully dense, non-faceted 111-textured high power impulse magnetron sputtering TiN films grown in the absence of substrate heating and bias. *Thin Solid Films 518*(21), 5978–5980.

Layes, V., C. C. Roca, S. Monje, V. Schulz-von der Gathen, A. von Keudell, and T. de los Arcos (2018). Connection between target poisoning and current waveforms in reactive high power impulse magnetron sputtering of chromium. *Plasma Sources Science and Technology 27*(8), 084004.

Leosson, K., S. Shayestehaminzadeh, T. K. Tryggvason, A. Kossoy, B. Agnarsson, F. Magnus, S. Olafsson, J. T. Gudmundsson, E. B. Magnusson, and I. A. Shelykh (2012). Comparing resonant photon tunneling via cavity modes and Tamm plasmon polariton modes in metal-coated Bragg mirrors. *Optics Letters 37*(19), 4026–4028.

Lundin, D., J. T. Gudmundsson, N. Brenning, M. A. Raadu, and T. M. Minea (2017). A study of the oxygen dynamics in a reactive Ar/O_2 high power impulse magnetron sputtering discharge using an ionization region model. *Journal of Applied Physics 121*(17), 171917.

Magnus, F., A. S. Ingason, S. Olafsson, and J. T. Gudmundsson (2012). Nucleation and resistivity of ultrathin TiN films grown by high power impulse magnetron sputtering. *IEEE Electron Device Letters 33*(7), 1045 – 1047.

Magnus, F., O. B. Sveinsson, S. Olafsson, and J. T. Gudmundsson (2011). Current-voltage-time characteristics of the reactive Ar/N_2 high power impulse magnetron sputtering discharge. *Journal of Applied Physics 110*(8), 083306.

Magnus, F., T. K. Tryggvason, S. Olafsson, and J. T. Gudmundsson (2012). Current-voltage-time characteristics of the reactive Ar/O_2 high power impulse magnetron sputtering discharge. *Journal of Vacuum Science and Technology A 30*(5), 050601.

References

Moreira, M. A., T. Törndahl, I. Katardjiev, and T. Kubart (2015). Deposition of highly textured AlN thin films by reactive high power impulse magnetron sputtering. *Journal of Vacuum Science and Technology A 33*(2), 021518.

Raadu, M. A., I. Axnäs, J. T. Gudmundsson, C. Huo, and N. Brenning (2011). An ionization region model for high power impulse magnetron sputtering discharges. *Plasma Sources Science and Technology 20*(6), 065007.

Sarakinos, K., J. Alami, C. Klever, and M. Wuttig (2008). Process stabilization and enhancement of deposition rate during reactive high power pulsed magnetron sputtering of zirconium oxide. *Surface and Coatings Technology 202*(20), 5033 – 5035.

Shimizu, T., M. Villamayor, D. Lundin, and U. Helmersson (2015). Process stabilization by peak current regulation in reactive high-power impulse magnetron sputtering of hafnium nitride. *Journal of Physics D: Applied Physics 49*(6), 065202.

Suresh Babu, S., J. Fischer, M. Rudolph, D. Lundin, and J. T. Gudmundsson (2024). Modeling of high power impulse magnetron sputtering discharges with a zirconium target. *Journal of Vacuum Science and Technology A 42*(4), 043007.

Toneli, D. A., R. S. Pessoa, M. Roberto, and J. T. Gudmundsson (2015). On the formation and annihilation of the singlet molecular metastables in an oxygen discharge. *Journal of Physics D: Applied Physics 48*(32), 325202.

Vlček, J., J. Rezek, J. Houška, R. Čerstvý, and R. Bugyi (2013). Process stabilization and a significant enhancement of the deposition rate in reactive high-power impulse magnetron sputtering of ZrO_2 and Ta_2O_5 films. *Surface and Coatings Technology 236*, 550–556.